energies

MDPI

Article

Solar-DG and DSTATCOM Concurrent Planning in Reconfigured Distribution System Using APSO and GWO-PSO Based on Novel Objective Function

Bikash Kumar Saw [1], Aashish Kumar Bohre [1], Jalpa H. Jobanputra [2] and Mohan Lal Kolhe [3,*]

[1] Department of Electrical Engineering, National Institute of Technology, Durgapur 713209, India
[2] Electrical Engineering Department, Shroff S R Rotary Institute of Chemical Technology, UPL University of Sustainable Technology, Ankleshwar 393135, India
[3] Faculty of Engineering and Science, University of Agder, 4604 Kristiansand, Norway
* Correspondence: mohan.l.kolhe@uia.no; Tel.: +47-93414532

Abstract: The concurrent planning of multiple Distributed Generations (DGs), consisting of solar-DG and DSTATCOM with reconfiguration in IEEE 33 and 69 bus Radial Distribution Network (RDN), using Adaptive Particle Swarm Optimization (APSO) and hybrid Grey Wolf-Particle Swarm Optimization (GWO-PSO), is reported in this paper. For this planning, a novel multiple objective-based fitness-function (MO_F^F) is proposed based on various performance parameters of the system, such as power losses (both active, as well as reactive loss), system voltage profile, short circuit level of line current ($SCLL_{Current}$), and system reliability. The economic perspective of the system has also been considered based on the various costs, such as fix, loss, and Energy Not Supplied (ENS) cost. Two case studies have been presented on IEEE 33 and 69 bus RDN to validate the efficacy of the proposed methodology. The results analysis of the system shows that better performance can be achieved with the proposed technique for 33 and 69 bus RDN, using GWO-PSO rather than APSO. From this results analysis, a vital point is noticed that the $SCLL_{Current}$ is reduced, which causes the short-circuit (fault) tolerance capacity (level) of the RDN to become enhanced. Finally, the comparative analysis of the obtained results, using the proposed method with other methods that exist in different literature, reveals that the proposed method has performed better from a techno-economic prospective.

Keywords: solar distributed generation (Solar-DG); distribution static compensator (DSTATCOM); reconfiguration tie-switching (TS); distribution system planning; APSO; GWO-PSO

Citation: Saw, B.K.; Bohre, A.K.; Jobanputra, J.H.; Kolhe, M.L. Solar-DG and DSTATCOM Concurrent Planning in Reconfigured Distribution System Using APSO and GWO-PSO Based on Novel Objective Function. *Energies* **2023**, *16*, 263. https://doi.org/10.3390/en16010263

Academic Editor: Abu-Siada Ahmed

Received: 20 November 2022
Revised: 15 December 2022
Accepted: 22 December 2022
Published: 26 December 2022

1. Introduction

A power system has mainly four parts: generation sector, transmission sector, distribution sector, and utility sector/ends. The distribution sector is a vital part among all the four parts of the power system. This sector suffers from a massive amount of losses related to power (real power losses-P_{Loss} and reactive power losses-Q_{Loss}) and deviation in voltage (V_D), with system reliability (R_S) issues. These need to be minimized by applying heuristic optimization techniques. This will maintain the short circuit level of line current and economy of the system. Consequently, it will improve the operation and control of the system. Varied kinds of solution methods are available, among which concurrent multiple DG planning and concurrent multiple DG planning with reconfiguration in RDN are proposed in this paper, as they are superior to others. Only DG planning and DG planning with reconfiguration through tie switches will enhance the profile of the voltage, fault (short circuit) current tolerance capacity, or level, as well as the reliability of the RDN.

This is because, through this planning approach, the reduction in system power losses and $SCLL_{Current}$ can be achieved. At the same time, the considered economic factors, such as fix, loss, and ENS cost, will also reduce. The IEEE 33-bus and 69-bus RDN are considered

to validate the proposed approach. The RDNs are the least expensive and simplest for their construction and protection scheme; these networks never make any loop for their radial nature. Therefore, it is important to maintain network radiality. While performing the reconfiguration, the radiality of the distribution network must be maintained so that the distribution network will not make any loop.

1.1. Literature Survey

In [1], the planning of solar-DG and DSTATCOM in IEEE 118 and 69-bus RDN, using Ant Lion Optimizer (ALO) and Modified ALO (MALO), considering seasonal load variation with solar-irradiance to optimize the total annual cost, bus voltage deviation, and stability. In the article, Ref. [2] the author allocates DSTATCOM and PV in the IEEE 30-bus system to reduce the real power loss, using the Fuzzy Lightning Search Algorithm (Fuzzy LSA). The system reconfiguration and objective parameters, such as Q_{Loss}, R_S, and $SCLL_{Current}$, can also be included for the considered system planning in both of the above literature. In the proposed work, technical and economic objectives, along with social objectives, such as benefit-cost ratio, emission cost-benefit, and voltage profile enhancement indices, are considered for the optimal location and size of DG and DSTATCOM, using PSO with adaptive inertia weight [3]. In addition to these objectives, the P_{Loss}, Q_{Loss}, R_S, and $SCLL_{Current}$ can also be considered for this planning. In [4], the target is to enhance techno-economic benefit through improving system voltage and reducing line losses, along with the pollutants emission, using the Improved Crow-Search Algorithm (Improved-CSA) for planning different Renewable Energy Sources (RES) and DSTATCOM in the 51-bus practical distribution network, considering variable load. Here, the authors found that the planning of different devices is better in weaker buses as compared to the healthier buses with respect to computational time and algorithm performance. Parameters such as R_S and $SCLL_{Current}$ with system reconfiguration have not considered in this work.

In [5], it is concluded that compensating the real and reactive power using DG and DSTATCOM integration with Cuckoo Search Algorithm (CSA) leads to improvement in overall energy efficiency, power quality, voltage profile, power factor, load balancing, and system stability. Along with this power loss, on-peak operating costs and pollutant emissions of IEEE 12-bus, 34-bus, and 69-bus RDN are minimized. In this work, many techno-economic perspectives are addressed, but Q_{Loss}, R_S, and $SCLL_{Current}$ can also be addressed here. In [6], with variable load and uncertainty of DG output, the DGs and DSTATCOM are allocated using fuzzy logic-based Rooted Tree Hybrid Optimization (fuzzy logic RTO) to improve the profile of voltage, economic, and environmental benefits with a reduction in losses on 118 and 69-bus RDNs, which is investigated. The optimal size and optimal allocation of DSTATCOM utilizing the bat algorithm, based on the voltage stability index, for the reduction in a power loss of 33 and 69-bus RDN is presented in [7]. In [8], the revealed result indicates that the proposed objective has been achieved with 75.93% and 44.71% as loss reduction, 51.76% and 33.2% as voltage profile improvement, and 36.42% and 33.2% as load balancing, respectively, for both the considered IEEE Tai-Power 11.4 kV and 33-bus distribution network. In addition, network reconfiguration can also be done in [6,7], whereas the proposed work of [6–8] can be extended further, considering the R_S and $SCLL_{Current}$ as other indices.

The simulation results of all three cases using Extended Nondominant Sorting Genetic Algorithm II (Extended NSGA II) reveal that planning of PV with Battery and DSTATCOM maximizes the objective parameters by maintaining all security constraints, such as power flow, voltage unbalance, and power factor, as given in [9]. The presented work can also be extended and validated by including P_{Loss}, Q_{Loss}, and $SCLL_{Current}$, with other factors of reliability instead of ENS only. The integration of biomass and intermittent renewable DGs with capacitor banks in 94-bus Portuguese RDN is proposed in [10], where the objective has been achieved with the reduction in P_{Loss} up to 77.82%, voltage stability index 44.25%, and V_D 9.68% [10]. The disadvantage of this work is only RDGs are planned with three technical parameters; it can be improved by considering more parameters with reconfiguration.

In [11], the author has taken three objective indices—maximization of voltage stability index, reduction of P_{Loss}, and total V_D—with DG and DSTATCOM planning, using LSA in 33 and 69-bus RDN. In [12], the author proposes optimal planning of single DG and single DSTATCOM at bus number 13 of 33-bus IEEE RDN, which reduces the reactive and real power loss up to 95.3274 KVAr and 121.7023 kW, respectively, using an analytical approach. Again in [13], the authors have optimally placed DG and DSTATCOM with 18.94 kW and 31.94 kW reduction in losses of power with an enhanced voltage profile using the Evolutionary-based Bat Algorithm (EA based BA) of Standard 34 and 85-bus IEEE system [13]. The authors of [11–13] tried to achieve the objective with DG and DSTATCOM planning only; its efficacy can be extended further by considering reconfiguration also.

The result in [14] proves that network reconfiguration with DSTATCOM and PV leads to a significant reduction in power loss, with voltage profile enhancement of IEEE 33, 69, and 118 bus RDN, using the Grasshopper Optimization Algorithm (GOA). The results of [15] prove that optimal planning of DG and DSTATCOM leads to a significant reduction in power losses, with voltage profile enhancement using CSA in IEEE 33 and 136 bus RDN. In [16], the outcome states that optimal planning of DG and DSTATCOM leads to a significant enhancement in voltage profile, as well as the reduction in power loss, using the Loss Sensitivity Factor (LSF) and Hybrid Lightning Search Algorithm-Simplex Method (Hybrid LSA-SM) for both IEEE 33 and 69-bus RDN. In [17], the author proposed an approach to reduce daily real power loss with an enhanced profile of the voltage in the presence of PEV, with a daily variation of load using PSO and Butterfly Optimization (BO) by planning DG in a 33-bus RDN. By only optimizing the P_{Loss} and V_D, the effectiveness and robustness of the proposed work [14–17] cannot be justified; more technical parameters have to be considered for optimization.

The proposed work of [18], is tested in three IEEE systems, namely, 33, 69-bus, and a Practical Brazil 136-bus, using Student Psychology-Based Optimization (SPBO) for their optimal DG allocation solution. Finally, note that SPBO helps in the minimization of P_{Loss} and V_D with less computational time and rate of prominent convergence. Furthermore, this work can be expanded by considering other parameters along with system reconfiguration. In the literature [19–22], the Grey Wolf Optimization (GWO) and hybrid GWO-PSO algorithm are applied to the optimization problem. In [23–25], the bus injection to branch current and branch current to bus voltage (BIBC-BCBV)-based, backward-forward, sweep load, flow (LF) technique is explained for RDN load flow analysis (LFA). The Mixed Integer Non-Linear Programming (MINLP)-based optimization approach is used in IEEE 69 and 33-bus RDN for the planning of DGs to mitigate the losses with an enhanced profile of voltage in [26]. This work can be implemented further by using other optimization techniques, considering different techno-economic parameters along with the considered one. In [27–30], the authors proposed various techniques for DG planning in the distribution sector. The planning of these DGs will enhance the overall system performance in terms of operation, economy, and reliability. The optimization technique called PSO (Particle Swarm Optimization technique) and APSO (Adaptive PSO) are illustrated in [27,28], respectively, using them for DG planning. The technologies available for DG to harvest renewable energy near the load end are listed in [29]. In [30], using the Genetic Algorithm (GA) and PSO planning of multiple DGs with different load models was presented. The IEEE 33 and 69-bus RDN with 54-bus practical system is considered for the validation of results. It is noticed that there is significant reduction in losses, ENS, and apparent power intake, with enhancement of the voltage profile, system reliability, benefit in cost, and transfer capacity. However, a major drawback is that for reliability index calculation, only ENS is taken into account; hence, other interruptions related to reliability can also be considered for further analysis, including network reconfiguration with $SCLL_{Current}$.

The author of [31] reveals that the suggested approach using PSO is capable of integrating multiple DGs with different load models, but the impact of network reconfiguration was not considered. This planning has been carried out to decrease the losses, MVA flows, and intake from the grid, along with improvement of the voltage stability margin and

loading for 38- and 30-bus systems. The work [32] presents a multi-objective index for IEEE 34-bus medium voltage RDN with time-varying DGs. This includes wind speed and hourly demand, which constitute various technical aspects, such as P_{Loss}, Q_{Loss}, V_D, reverse conductor capacity, and single and three phase-to-ground short circuits. The author of [33] proposed an optimal planning of DGs, using the GA and Bat Algorithm (BA) and its comparative analysis to optimize the index for P_{Loss} and voltage stability, but did not consider DG planning; hence, it can be considered further. The work [34] introduces P_{Loss} and reliability indices minimization as an objective with the reconfiguration of RDN, using the Imperialist Competitive Algorithm (ICA) without considering any kind of DGs or other technical parameters. In [35], the characterization of DG is presented based on their power injection. In [36], different IEEE test system data and load flow techniques are presented. The author of [37] applied a unique codification of GA for reconfiguration of 69-, 84-, and 135-bus systems to minimize loss. By using PSO, the reconfiguration of IEEE 33 and 69-bus RDN is proposed in [38]. The authors of [37,38] only considered reconfiguration planning for loss and V_D minimization without DG.

The various concepts related to DG types and their implementation using different techniques to improve the system parameters are discussed in [39–42]. Here, only P_{Loss} and Q_{Loss} were taken into consideration in the planning of DGs without system reconfiguration. The planning of the grid-connected and isolated hybrid renewable energy system (HRES), including solar PV and wind systems, are explained in [43–46]. These works only focused on HRES implementation with economic and environmental parameters impacts, without considering any impact of technical parameters. Strategic optimum planning of solar, along with battery and FACTS devices, with its modelling is given in [47–50]. The author of [47] optimized a reliability index by only considering a single interruption, which was ENS. In [51], the planning of DG is carried out using an Evolutionary Algorithm (EA) to mitigate losses and total-harmonic distortion in voltage. Implementation of DG in an optimized reconfigured network, using the PSO and Dragonfly Algorithm (DA) [52], the dataset approach, and the Water Cycle Algorithm (WCA) [53], FA, and EA [54] are presented. In [51–54], the major drawback was in DG planning with reconfiguration, because the only technical parameters considered as objective were P_{Loss}, V_D, and the total harmonic distortion in voltage. Hence, the planning of multiple DGs with and without reconfiguration is a challenging goal, based on the multiple objective-based fitness-function consisting of non-linear nature constraints.

The detailed review of distribution system planning, methodology, objectives, and outcomes based on different literature are tabulated in Table 1. From this detailed review, it is found that none of the authors have considered the proposed "novel multiple objective-based fitness-function" for the "concurrent optimal planning of multi solar-DG and DSTATCOM with and without reconfiguration". Therefore, this work is carried out efficiently using the APSO and GWO-PSO techniques, in which two proposed cases have been studied: Proposed Case-1 (PC-1)—Concurrent optimal planning of multi solar-DG and DSTATCOM without the impact of RDN reconfiguration, and Proposed Case-2 (PC-2)—Concurrent optimal planning of multi solar-DG and DSTATCOM with the impact of RDN reconfiguration.

Table 1. Review on Distribution System Planning Methodology, Objectives, and Outcomes.

Author's	Objectives	Method	System	Load Type	Distribution System Planning	Outcomes
Oda et al., 2021 [1]	The objective is to minimize total annual cost, V_D and maximize system stability.	ALO and MALO	Standard 69 and 118-bus IEEE system	Seasonal load	Planning of Solar-DG and DSTATCOM	The result of the proposed work reveals that the objective has been achieved by reducing the total annual cost, V_D with enhanced R_S.

Table 1. *Cont.*

Author's	Objectives	Method	System	Load Type	Distribution System Planning	Outcomes
Isha et al., 2021 [2]	To increase voltage stability with decrement V_D and P_{Loss}.	Fuzzy LSA	Standard IEEE 30 bus RDN	C_{Load}	Siting and Sizing of DSTATCOM and Solar-DG	From the comparative analysis of the work, it is found that the objective has been achieved.
Ghatak et al., 2017 [3]	The objective is to maximize the benefit-cost ratio, emission cost-benefit with profile of voltage improvement indices.	PSO with Adaptive Inertia weight	Standard 33 and 69-bus IEEE system	C_{Load}	Planning of DG and DSTATCOM	The result analysis reveals that the objective is achieved with better computational efficiency in the unhealthy case of the RDN as compared to the healthy case.
Sannigrahi et al., 2019 [4]	The target is to improve economic benefit, system voltage and decrease pollutants emission with line losses.	ICSA	51-bus practical distribution network	VR_{Load}	Integration of Renewable Energy Sources and DSTATCOM	The outcomes state that the objective is achieved with reduced computational time and improved algorithm performance for the weaker buses of the practical distribution system as compared to the healthier buses.
Yuvaraj et al., 2017 [5]	To minimize a problem formulated for reduction in total loss of power with respect to different equality and inequality constraints.	CSA	Standard IEEE 12, 34, and 69-bus RDN	C_{Load}	Integration of DG and DSTATCOM	Compensating the real and reactive power using DG and DSTATCOM integration with CSA leads to improvement in overall energy efficiency, power quality, voltage profile, power factor, load balancing, system stability, etc.
Sannigrahi et al., 2019 [6]	To improve the economic and environmental benefits with profile of voltage, and reduction in losses.	Fuzzy Logic–based RTO	Standard IEEE 69, and 118 bus system	VR_{Load} with uncertainty in DG output	Integration of DG with DSTATCOM	In this work, the DG and DSTATCOM are planned taking varying load and uncertainty of DG output to improve the economic and environmental benefits with profile of voltage and reduction in losses.
Yuvaraj et al., 2017 [7]	To decrease the loss of power balancing is taken as objective.	BA	Standard 33 and 69-bus IEEE system	C_{Load}	Planning of DSTATCOM	In this work BA along with voltage stability index is utilized for the optimal allocation and sizing of DSTATCOM separately for the reduction in power loss of RDN.

Table 1. *Cont.*

Author's	Objectives	Method	System	Load Type	Distribution System Planning	Outcomes
Tolabi et al., 2014 [8]	Reduction in loss of power with increased voltage profile and feeder load balancing is taken as objective.	Fuzzy-Ant Colony Optimization (Fuzzy-ACO)	Tai-Power 11.4 kV real and 33-bus IEEE RDN	VR_{Load} (Light, Normal and Heavy)	Simultaneous reconfiguration planning with DG and DSTATCOM	The revealed result says that the objective has been achieved with 75.93% and 44.71% as loss reduction, 51.76% and 33.2% as voltage profile improvement, respectively for both the considered systems.
Ghatak et al., 2020 [9]	The aim is to enhance economic, environmental, technical, and reliability characteristics.	Extended NSGA II	Three-phase practical unbalanced 240-node USA system	VR_{Load}	Planning of PV with Battery and DSTATCOM	The simulation results of all three cases reveal that planning of PV with Battery and DSTATCOM (case 3) maximizes the objective parameters.
Malik et al., 2020 [10]	The objective is to optimize indices of voltage stability, power losses, and V_D.	PSO	Portuguese 94-bus distribution system	VR_{Load}	Intermittent renewable DGs planning with biomass and capacitor banks	Planning of DGs with biomass and capacitor banks in 94-bus Portuguese RDN is proposed, where the objective has been achieved with reduced power loss and VD up to 77.82% and 9.68%.
Thangaraj et al., 2017 [11]	To enhance the index for voltage stability and minimize the index for power loss, V_D.	LSA	Standard 33 and 69-bus IEEE system	Light (0.5) to Peak (1.6) load	Planning of DG and DSTATCOM	Three objective indices were considered by the author and the same was achieved with DG and DSTATCOM planning using LSA in 33 and 69-bus RDN.
Weqar et al., 2018 [12]	Power loss and V_D minimization.	Analytical approach	33-bus IEEE RDN	C_{Load}	DSTATCOM and DG planning	Author proposes optimal planning of single DSTATCOM and DG at bus number 13 of 33-bus IEEE RDN, which reduces the active and reactive loss of power to 121.7023 kW and 95.3274 kVAr.
Salkuti et al., 2021 [13]	Aim is to decrease the loss of power and enhance the voltage profile.	EA based BA	Standard 34 and 85-bus IEEE system	C_{Load}	Planning of DG and DSTATCOM	Here the author optimally placed DG and DSTATCOM with reduced loss of power with enhanced voltage profile.
Sambaiah et al., 2020 [14]	The power loss reduction and profile of voltage improvement is taken as objective.	GOA	IEEE 33, 69, and 118 bus system	VR_{Load}	Optimal reconfiguration planning with DG and DSTATCOM	The result proves that network reconfiguration with DSTATCOM and PV leads to reduction in power loss and voltage profile improvement.
Yuvaraj et al., 2020 [15]	Aim is to decrease the loss of power and enhance the voltage profile.	Bio-Inspired CSA	IEEE 33, and 136-bus system	VR_{Load}	DSTATCOM and DG planning	In this work, the result proves that planning of DG and DSTATCOM leads to decrement in loss of power, as well as voltage profile enhancement using CSA.

Table 1. *Cont.*

Author's	Objectives	Method	System	Load Type	Distribution System Planning	Outcomes
Chinnaraj et al., 2020 [16]	The target is power loss minimization and voltage profile improvement.	LSF and LSA-SM	Standard 33 and 69-bus IEEE system	C_{Load}	Allocation of DG and DSTATCOM	The outcome states that allocation of DSTATCOM and DG reduces loss of power, as well as the profile of voltage enhancement using LSA-SM for both IEEE 33 and 69-bus RDN.
Injeti et al., 2020 [17]	The objective is to minimize everyday P_{Loss}, along with improvement in the profile of voltage.	PSO and BO	IEEE 33-bus RDN	VR_{Load}	In presence of Plug-In Electric Vehicle (PEV) integration of DGs	The author proposed an approach to reduce daily real power loss with an enhanced profile of the voltage in presence of PEV using PSO and BO by planning DG in a 33-bus RDN.
Balu et al., 2021 [18]	To minimize V_D, P_{Loss}, and voltage stability index.	SPBO	IEEE 33 and 69 bus RDN with real 136 bus system	VR_{Load}	Optimal integration of DG	The proposed work is tested in three systems, and for all the systems SPBO is applied for their optimal DG allocation solution. Finally noticed the optimal solution.
Alam et al., 2018 [26]	The objective is to mitigate loss, with enhancement in voltage profile.	MINLP	Standard 33 and 69-bus IEEE system	C_{Load}	Integration of distributed generation	Outcomes of the two test systems signify the impacts of the proposed approach aiming to reduce losses with enhancement in voltage profile by integrating DG optimally.
Bohre et al., 2016 [30]	To minimize a function comprises of losses, voltage profile, reliability, and shift factor indices.	GA and PSO	Standard 54-bus real system with 33 and 69-bus IEEE RDN	C_{Load}, IN_{Load}, RES_{Load}, COM_{Load}, MIX_{Load}	Integration of multiple DGs with different models of load	The systems results signify a reduction in losses, ENS, apparent power intake with enhancement in voltage profile, system reliability, benefit in cost, and ATC.
El-Zonkoly, A.M. 2011 [31]	Optimizing an objective function comprises of P_{Loss} and Q_{Loss}, voltage profile, intakes in MVA and line loading.	PSO	38-bus radial and 30-bus meshes system	C_{Load}, IN_{Load}, RES_{Load}, COM_{Load}, MIX_{Load}	Integration of multiple DGs with different models of load	The outcomes reveal that the suggested approach is capable of integrating multi-DGs with different models of load to decrease the losses, MVA flows and intake from the grid, along with voltage stability margin and loading improvement.
Prakash et al., 2016 [33]	Aim is to decrease the P_{Loss} and improve the index for voltage stability.	BA	Standard 69-bus IEEE system	C_{Load}	Integration of distributed generation	The noticed result clarified that using BA the objective has been achieved with an improved profile of voltage.

Table 1. *Cont.*

Author's	Objectives	Method	System	Load Type	Distribution System Planning	Outcomes
Sedighizade et al., 2017 [34]	To minimize indices of reliability and $P_{Loss.}$	ICA	Standard 33 and 69-bus IEEE system	C_{Load}	Network reconfiguration	Outcome reveals that the objective has achieved with minimized real power loss and increased reliability.
Prakash, et al., 2016 [35]	Objective is to decrease power loss, along with increment in profile of voltage.	PSO	Standard 33 and 69-bus IEEE system	C_{Load}	Integration of distributed generation	Through this effective work, the decrement in power loss, along with increment in the profile of voltage takes place.
Swarnkar et al., 2011 [37]	Objective is to minimize the loss.	GA	IEEE 69, 84 and 135 bus system	C_{Load}	Network reconfiguration	Through the proposed method, the loss has been minimized and validated on all the three considered systems.
Reddy et al., 2016 [38]	The objective is to decrease P_{Loss} and V_D.	PSO	Standard 33 and 69-bus IEEE system	VR_{Load} (Light, Normal and Heavy)	Network reconfiguration	Through this effective work, the decrement in real power loss, along with increment in the profile of voltage at poor buses above 0.9 p.u. take place.
Ghatak et al., 2018 [47]	The target is to maximize technical, economical, reliable and environmental features of the system considered.	E_NSGA II	Standard 69-bus IEEE system	VR_{Load}	Integration of Renewable Energy Resources, Battery Storage Systems and DSTATCOM	Through this approach, the technical, economical, reliable and environmental features of the system have been maximized. To check the efficacy of revealed outcomes, the said approach has been compared with other multiple-objective-based approach.
Taher et al., 2014 [48]	Objective is to reduce power loss with minimum cost of DSTATCOM installation by considering enchantment of current and voltage profile.	Immune Algorithm	Standard 33 and 69-bus IEEE system	VR_{Load} (Light, Medium and Peak)	Optimal integration of DTATCOM	Noticed results say that the target is achieved with reduced loss of power and cost of installation for DSTATCOM, improved current profile, and voltage profile of buses.
Kadir et al., 2013 [51]	The objective is to reduce power loss with total harmonic distortion in voltage	EA	Standard 69-bus IEEE system	C_{Load}	Integration of distributed generation	The outcomes reveal a reduction in total harmonic distortion in voltage and losses with the improved voltage profile.

Table 1. *Cont.*

Author's	Objectives	Method	System	Load Type	Distribution System Planning	Outcomes
Vempalle et al., 2020 [52]	To maximize the savings on DG installation, maintenance cost and minimize the loss.	PSO and DA	IEEE 33 and 69 bus system	C_{Load}	Optimal Reconfigure using PSO with DG Planning using DA	In this work using hybrid PSO-DA, the optimal planning of DG with reconfiguration is carried out, and the outcomes show maximization of savings with reduction in loss.
Muhammad et al., 2019 [53]	The aim is to enhance the RDN planning via its reconfiguration and integration of DG to reduce the loss and enhance the RDN solution quality.	Dataset approach with WCA	Standard IEEE 33 and 69 bus RDN	C_{Load}	Reconfiguration, sizing and siting of DG	Depending on the evaluation from outcomes it is noticed that the power loss is reduced by 75.16% and 84.42% for IEEE 33 and 69-bus RDN respectively, also improves solution quality of considered networks via Network Reconfiguration and DG Integration.
Rahim et al., 2019 [54]	Objective is to keep the protective devices in coordination after planning with minimum P_{Loss} and V_D.	FA and EA	IEEE 33, 69, and 118 bus system	C_{Load}	Reconfiguration with DG incorporating protective devices	The outcomes reveal that the optimal reconfiguration and DG sizing with minimum P_{Loss} and V_D ensured coordinated protective devices operated correctly during normal and fault conditions.

1.2. Contribution of Paper

The novelty and major contributions reported in this paper are as follows:

1. A novel "multiple objective-based fitness-function" (MO_F^F) is proposed, as given in (10). This MO_F^F consists of five significant performance indices: real power loss, reactive power loss, system voltage profile, short circuit level of line current, and system reliability.
2. The short-circuit (fault) current tolerance capacity or level improvement factor is considered in the MO_F^F as a short circuit level of line current ($SCLL_{Current}$).
3. The economic perspective of the system has also been considered, based on the various costs, such as fix, loss, and energy not supplied (ENS) cost.
4. The novel MO_F^F is optimized for the optimal DG sizes and locations with optimal reconfiguration tie-switches, using the two optimization techniques, i.e., APSO and GWO-PSO.
5. To validate the proposed work efficacy, a techno-economic comparative result analysis has been presented for IEEE 33 and 69-bus RDN. In addition, the results are compared to other recent literature.

1.3. Paper Layout

This paper consists of six sections. The Section 1 is the Introduction, which describes the reviews related to DG technology, DG planning, and reconfiguration of distribution networks. The Section 2 is related to Distributed Generation and Related Different Technolo-

gies, associated with various DG technology and their application. The Section 3 includes the Modelling of Proposed System, including renewable solar-DG and DSTATCOM. The Section 4 presents the Proposed Methodology for the presented work. The Section 5 is Results and Discussion, which gives a detailed discussion related to 33- and 69-bus RDNs, based on the proposed methodology. The comparison with other methods is also done in the Section 5. The Section 6 is the Conclusion, which concludes the presented work based on different parameters, as proposed in the work.

2. Distributed Generation (DG) and Related Different Technologies

DG is defined as the power production/generation units located near the consumer end and directly connected with the utility. The implementation of DG technology offers a viable alternative to the traditional sources of electric power for applications, such as residential, commercial, and industrial, as presented in [23,29,30].

2.1. Distributed Generation

2.1.1. The Motivational Factors behind Distributed Generator/Resources Planning Are

- Its availability in an enormous amount with a vast range of resources
- The system reliability will improve after DG plantation
- Increment in system efficiency
- Reduction in system losses
- Improvement in the profile of voltage
- Total intake of power flow from the system will minimize
- Sudden load management is possible, rapidly and effectively
- Continuity in power supply improves
- Reduces the occurrence of interruption, failure, and any kind of risk
- Increment in Available Transfer Capacity (ATC) of the system
- Enhances the operation, availability of power, and economy
- Reduces loading of the transmission and distribution sector
- Reduction in toxic gases emission

2.1.2. The Concerns/Issues Defining Distributed Generators/Resources Are

- Purpose of DGs
- Location of DGs
- Rating/Capacity of DGs
- Area to deliver power by the DGs
- Technology adopted during DGs selection
- Impact of environmental condition on DGs
- Operational mode of the DGs
- The DGs owned by which body/ The DGs ownerships
- Penetration level of DG resources

2.1.3. On the Basis of Capacity to Deliver the Energy, the DG Units Are Named as

- Dispatchable, e.g., Small hydro plants, Gas-turbine based on biomass, and so on.
- Non-Dispatchable, e.g., generation depends on weather, such as solar and wind.

2.2. Different Technologies Related to DGs

The categorization of DG technology, based upon the power delivering capacity per module and their efficiency ranges, is illustrated in Table 2. DG technology can be classified, based on the operating range in which it can produce the output power within a specific limit under different types, as given in Table 3. Additionally, the different types of DG technologies, on the basis of design suitability for the use of various applications, are shown in Figure 1.

Table 2. Various DG technology with their per module specification and efficiency range.

DG Technology		Per Module Typical Size Range	Range of Efficiency in %
Renewable	Wind-Turbine	200 W–3 MW	40–80
	Solar-PV	20 W–1000 kW	35–45
	Biomass	100 kW–20 MW	60–75
	Small-Hydro	5 kW–100 MW	90–98
	Micro-Hydro	20 kW–1 MW	90–98
	Geothermal	5 MW–100 MW	35–50
	Ocean-Energy	100 kW–1 MW	80–90
	Solar-Thermal	1 MW–80 MW	50–75
	Battery-Storage	500 kW–5 MW	70–75
Non-Renewable	Internal-Combustion-Engines	5 kW–10 MW	80–90
	Reciprocating-Engines	3 kW–6 MW	80–85
	Combustion-Turbine	1 MW–250 MW	80–90
	Hybrid-Fuel Cell	200 kW–20 MW	80–85
	Small-Fuel Cell	1 kW–300 kW	80–90
	Micro-CHP	1 kW–10 kW	75–89
	Automotive-Fuel Cells	30 kW–60 kW	80–90
	Micro-Turbines	35 kW–1 MW	80–85

Table 3. DG technology based on size.

Distributed Generation Type	Range of Power Generation
Micro-DGs	≈1 W < 5 kW
Small-DGs	5 kW < 5 MW
Medium-DGs	5 MW < 50 MW
Large-DGs	50 MW < 300 MW

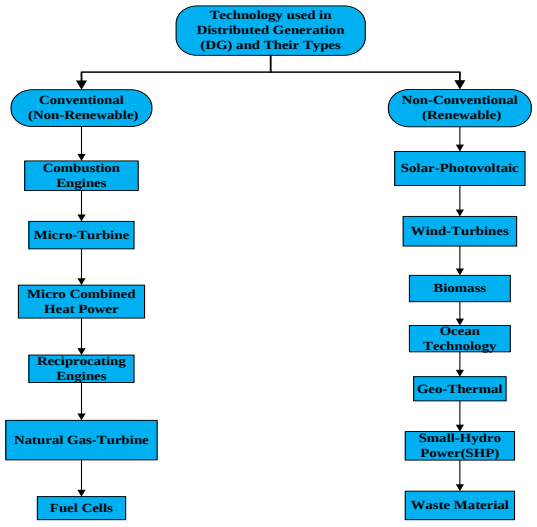

Figure 1. Different types of DG technology.

DG technology, based on its real and reactive power dispatch/supply or consumption capability, can be divided into four categories, as given in [30,35,39–41].

- DGs deliver real power only at the unity power factor (p.f.), known as Type-1. Example: photovoltaic (PV), micro-turbines, and fuel cells.
- Similarly, DGs deliver reactive power only at zero p.f., known as Type-2. Example: synchronous compensators, such as a gas turbine.
- Some of the DGs deliver real power, but absorb reactive power at optimum p.f. between 0 to 1. Example: induction generator (wind farm).
- Likewise, DGs deliver both real and reactive power at optimum p.f. between 0 to 1. Example: Synchronous generator (cogeneration, gas turbine, etc.).

3. Modelling of Proposed System

3.1. Modelling of Solar-DG or PV System (P_{RDG})

Solar energy is freely accessible in the atmosphere, and it is totally liberated from pollution. The output of solar PV depends on its geographic atmosphere. Its application for power production as a renewable source of power overcomes society's dependence on fossil fuels [43]. The power output of PV and its efficiency can be calculated with the help of (1) and (2), as mentioned [44].

$$P^{PV} = aG\eta^{PV} \tag{1}$$

$$\eta^{PV} = \eta^{STC}\left[1 + \alpha\left(T^{cell} - 25\right)\right] \tag{2}$$

where, P^{PV} is the power output of PV; "a" is the panel area in meters squared (m^2); and "G" is incident solar radiation, with the unit representation of watts per meters squared (W/m^2). η^{PV} and η^{STC} represent the efficiency in the determined operating condition and under Standard Test Conditions (STC). Cell temperature in °C is T^{cell}, and in percentage per °C temperature, the co-efficient "α" is represented. After merging (1) and (2), a new (3) and (4) are formulated. These developed equations will give the output power under STC.

$$P^{PV} = P^{STC}\left\{\frac{G}{100}\left[1 + \alpha\left(T^{cell} - T^{0}\right)\right]\right\} \tag{3}$$

$$T^{cell} = T^{am} + \left(\frac{T^{NOC} - 20}{800}\right)G \tag{4}$$

where T^{NOC} = nominal operating cell temperature in °C, T^{am} = ambient temperatures in °C, and T^{0} = 25 °C.

3.2. Modelling of DSTATCOM (Q_{DSTAT})

DSTATCOM is considered as Q_{DSTAT} for this work. It is a shunt-connected voltage-source converter, coupled with a medium- to low-voltage distribution framework. It has numerous advantages compared to a shunt-connected capacitor. It provides fast response, more governing capacity, less harmonic, and compatibility in RDN [46]. It performs two operations, namely, supplying and absorbing the reactive power in the network. When the coupling point's voltage is less than the actual voltage, it will supply reactive power, but it will absorb the same when it is greater than the actual voltage [47]. The DSTATCOM is comprised of a DC link capacitor, an inverter model, and an AC filter with a coupling transformer. When the system is overloaded, the compensating current is injected at the DSTATCOM-allocated bus to control the system voltage [48]. The DSTATCOM model and the one-line diagram of a distribution network for successive buses without DSTATCOM [49,50] are presented in Figures 2 and 3, respectively. Here, the considered network is a balanced network. The (R_k + iX_k) is the impedance of the line between the k and (k + 1) buses. Voltage and current phasor representation of the system without DSTATCOM is shown in Figure 4. The pre-specified loads connected at the buses are expressed by (P_k + iQ_k) and (P_{k+1} + iQ_{k+1}), where the voltages are V_k and V_{k+1}.

The voltage and current phasor representation of the system without DSTATCOM are illustrated in Figure 3. Their corresponding equation can be expressed as (5) by using KVL.

$$V_{k+1}\angle\phi_{k+1} = V_k\angle\phi_k - (\mathrm{R}_k + \mathrm{iX}_k)\mathrm{I}_k\angle\delta \quad (5)$$

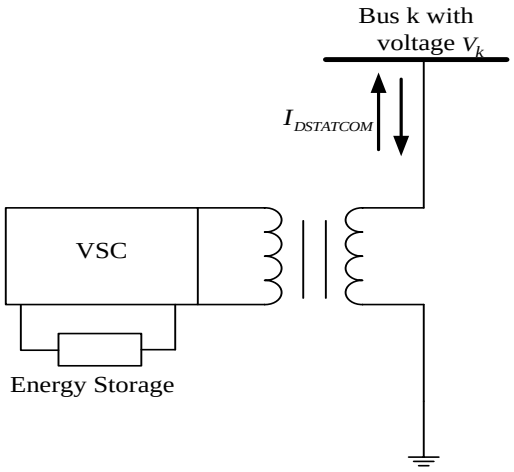

Figure 2. Typical Representation of DSTATCOM connected to kth Bus.

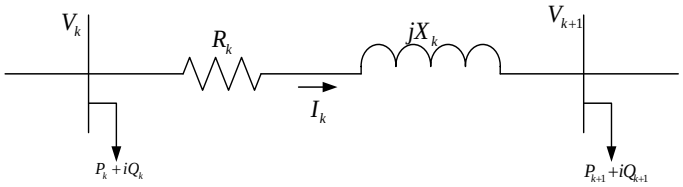

Figure 3. One-line diagram of a distribution framework for successive buses.

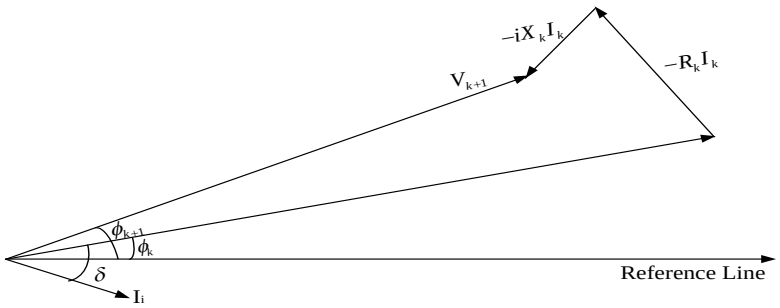

Figure 4. Voltage and current phasor representation of the system without DSTATCOM.

The applied load flow method in this work is BIBC-BCBV-based backward-forward sweep, which is used to derive all the variables. In a real system, the voltage of buses are less than 1 p.u.; therefore, the voltage at $(k + 1)$th bus is also 1 p.u. The installation of DSTATCOM is carried out for compensating the voltage at $(k + 1)$th bus and to maintain the required reactive power in the system, as shown in Figure 5. Hence, it can be said that in steady-state conditions, it is used for regulation of voltage, as well as to reduce the system losses and make the balance of the reactive power to the system the same for supplying and absorbing. The current injected by the DSTATCOM, i.e., ($\mathrm{I}_{\mathrm{DSTATCOM}}$), is in phase quadrature with reference to bus voltage, as shown in Figure 6.

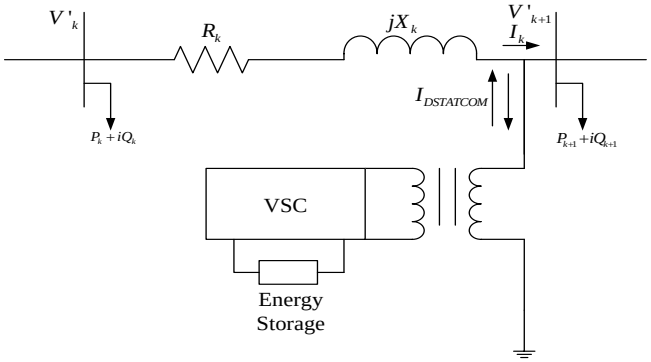

Figure 5. Installation of DSTATCOM in (k + 1)th bus of the system to be proposed.

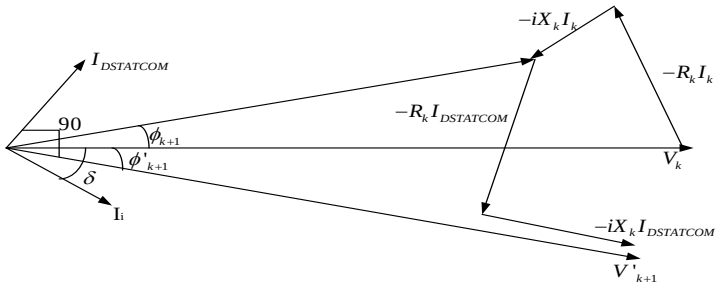

Figure 6. Voltage and current phasor representation of the system with DSTATCOM.

The equation for angle and voltage correction by injecting the DSTATCOM current is estimated as:

$$\angle I_{DSTATCOM} = \frac{\pi}{2} + \phi'_{k+1} \tag{6}$$

$$V'_{k+1}\angle\phi'_{k+1} = V'_{k}\angle\phi'_{k} - (R_k + jX_k)\left\{I_k\angle\delta + I_{DSTATCOM}\angle\left(\frac{\pi}{2} + \phi'_{k+1}\right)\right\} \tag{7}$$

The current I_k and $I_{DSTATCOM}$ flow simultaneously through the line/branch after installation of DSTATCOM in the (k + 1)th bus.

The reactive power injected by the DSTATCOM for system performance improvement, such as correction of voltage, at (k + 1)th bus till $V'_{(k+1)}$ is given by:

$$iQ_{DSTATCOM} = \left(V'_{k+1}\angle\phi'_{k+1}\right)\left\{I_{DSTATCOM}\angle\left(\frac{\pi}{2} + \phi'_{k+1}\right)\right\}^{*} \tag{8}$$

The current injected by DSTATCOM ($I_{DSTATCOM}$) and the angle change will be zero when the voltage is equal after and before the installation of DSTATCOM, i.e., $V'_{(k+1)} = V_{(k+1)}$. Mathematically, as a boundary condition, it is represented as:

$$V'_{k+1} = V_{k+1} \Rightarrow \begin{cases} I_{DSTATCOM} = 0 \\ \phi'_{k+1} = \phi_{k+1} \end{cases} \tag{9}$$

4. Proposed Methodology

4.1. Formulation of Multiple Objective-Based Fitness-Function

A novel multiple objective-based fitness-function (MO_F^F) is introduced in this section. This MO_F^F, as given in (10), consists of five significant operational and performance parameters as indices. The minimization of this unique MO_F^F is utilized for the optimal allocation of multi solar-DG as a real power DG and DSTATCOM as a reactive power DG. It also includes the impact of network reconfiguration by the incorporation of APSO and GWO-PSO techniques in IEEE 33 and 69-bus RDN. Hence, this remarkable novel MO_F^F is

used for the optimal positioning and sizing of multi DGs (solar-DG and DSTATCOM), with and without reconfiguration, by utilizing the APSO and GWO-PSO techniques.

$$MO_F^F = C_1 \times IP_{Loss} + C_2 \times IV_D + C_3 \times IQ_{Loss} + C_4 \times ISCC_{Line} + C_5 \times IR_S \quad (10)$$

Here, C_1, C_2, C_3, C_4, and C_5 represent the weight-factors with the weightage of 0.30, 0.25, 0.20, 0.15, and 0.10 separately. The elaborated concept of selecting the weight-factors is given in the literature [30–32]. These factors express exactly how much weight is given to every system variable attribute (indices). Their values are decided on the priority basis of individual indices' performance. It is significant while planning solar-DG and DSTATCOM, with and without reconfiguration impact, in an RDN.

IP_{Loss}, IV_D, IQ_{Loss}, $ISCLL_{Current}$, and IR_S are indexes for loss of real power, deviation in voltage, loss of reactive power, short circuit level of line current, and system reliability, respectively. In the novel MO_F^F, priorities are given to all the key factors that will upgrade the RDN to more reliable and effective. The main objective is to minimize the total loss of power (real and reactive) and deviation in voltage. Therefore, the highest weightage is given to the loss in real power (P_{Loss}), which is followed by deviation in voltage (V_D), and loss in reactive power (Q_{Loss}), with 30%, 25%, and 20% of weightage, respectively. Then, 15% and 10% weightage is given to the short circuit level of the line/branch current ($SCLL_{Current}$) and system reliability (R_S).

4.2. System Parameter Calculation

The calculation of the voltage and current of every bus and branch through backward-forward sweep LFA based on BIBC-BCBV matrices can be formulated as [24,25]:

- Each bus load current is expressed in (11):

$$L_C(i)^k = \left(\frac{P_L(i) + Q_L(i)}{V(i)^k}\right) \quad (11)$$

- Branch current determined by (12):

$$B_C = [BIBC][L_C] \quad (12)$$

- Each bus voltage can be updated by (13):

$$V_m = V_n - B_C(n-1) \times Z_{nm} \quad (13)$$

- The change in voltages at different buses can be evaluated by (14):

$$[\Delta V] = [BCBV][B_C] \quad (14)$$

- The apparent power loss can be determined by (15):

$$S_{Loss} = \sum_{j=1}^{N_B} [\Delta V][B_C]^* \quad (15)$$

- Calculation of P_{Loss} and Q_{Loss} is shown in (16), (17):

$$P_{Loss} = Real(S_{Loss}) \quad (16)$$

$$Q_{Loss} = Imag(S_{Loss}) \quad (17)$$

- Calculation of short circuit level of line current is shown in (18):

$$SCLL_{Current} = Max\left(\sum_{j=1}^{N}\sum_{\substack{i=2\\ j\neq i}}^{N} Y_{ji} \times (V_j - V_i)\right) \tag{18}$$

Calculation of MO_F^F indices are as follows:

- Index for loss of real power is given by (19):

$$IP_{Loss}^{\chi} = \frac{P_{Loss}^{\chi}}{P_{Loss}^{BC}}, \text{ Where, } \chi = \text{PC} - 1 \text{ and PC} - 2, \ BC = \text{Base Case} \tag{19}$$

- Index for loss of reactive power is given by (20):

$$IQ_{Loss}^{\chi} = \frac{Q_{Loss}^{\chi}}{Q_{Loss}^{BC}}, \tag{20}$$

- Index for deviation in voltage is shown in (21):

$$IV_D = max\left(\frac{\Delta V(n)}{v_{ref}}\right) \tag{21}$$

- Index for short circuit level of line current [31] is given by (22):

$$ISCLL_{Current} = \frac{SCLL_{Current}^{\chi}}{SCLL_{Current}^{BC}} \tag{22}$$

- The system reliability index calculation depends on its various parameters SAIFI, SAIDI, CAIDI, and ENS [30]:

$$SAIFI = \frac{\sum_{z=1}^{N} \gamma_z * MVA_z}{\sum_{z=1}^{N} MVA_z} \tag{23}$$

$$SAIDI = \frac{\sum_{z=1}^{N} UN_z * MVA_z}{\sum_{z=1}^{N} MVA_z} \tag{24}$$

$$CAIDI = \frac{SAIDI}{SAIFI} \tag{25}$$

$$ENS = \sum_{Z=1}^{N} MW_Z \times UN_Z \tag{26}$$

$$IR_S = \frac{Total\ Intrupted\ Power\ in\ MVA^{\chi}}{Total\ Intrupted\ Power\ in\ MVA^{BC}} \tag{27}$$

$$\text{Re}liability = 1 - \frac{Total\ Intrupted\ Power\ in\ MVA^{\chi}}{MVA_{Load\ Demand}} \tag{28}$$

where N and N_B = Number of total buses and branches; i and j = 2 to N and 1 to N_B; k is the kth iteration; L_C and B_C = Load and branch current at each bus and branch, respectively; V = Voltage at each bus; m = To-Bus; n = From-Bus, which is from 2 to N; γ_z and UN_z = Failure-rate and unavailability; MVA_z and MW_z = Each bus apparent and real power demand; and $MVA_{Load\ Demand}$ = Total connected apparent load.

The system cost parameters to calculate the capital recovery fixed cost, energy not supplied cost, and the energy loss cost are given as [30]:

- Capital recovery fixed cost (C_{FIX}) of system is shown in (29):

$$C_{FIX} = g \sum_{BR=1}^{N_{BR}} C_{BR} \tag{29}$$

- Cost for Energy Not Supplied is given by (30):

$$C_{ENS} = C_i \times ENS \tag{30}$$

- The cost of energy losses is shown in (31):

$$C_{LOSS} = 8760 \times C_l \times \phi \times \sum_{BR=1}^{N_{BR}} I_{BR}^2 \times R_{BR} \tag{31}$$

$$\phi = 0.15 \times \varphi + 0.85 \times \varphi^2 \tag{32}$$

where N_{BR}, I_{BR}, R_{BR}, C_{BR}, g, φ, and ϕ are the number of branches, branch current, resistance for the BRth branch, BRth branch cost of the main feeder, the yearly recovery rate of fixed cost, load factor, and loss factor, respectively. The C_i and C_l are p.u. cost of ENS and loss, respectively.

4.3. The Considered System with Different Cases

The two IEEE test networks, i.e., IEEE 33 and 69-bus RDN [37,38], as shown in, are considered in this work, with three cases as:

1. Base Case (BC): The system in which no modifications are considered for the proposed systems.
2. Proposed Case-1 (PC-1): This system includes the multi DGs as Solar-DG and DSTATCOM without Reconfiguration.
3. Proposed Case-2 (PC-2): This system includes the multi DGs as Solar-DG and DSTATCOM with Reconfiguration.

4.4. Adaptive Particle Swarm Optimization (APSO) Technique

The PSO and APSO were developed by Eberhart and Kennedy in 1995 [27] and Hue et al. in 2009 [28], respectively. PSO is a population-based technique for optimization. In its search space for each iteration, the particle will obey a specified velocity and inertia. The development of PSO to APSO takes place with some adjustments in PSO parameters, such as inertia weight, and then the incorporation of the extra constriction factor (ρ). Hence, these changes in PSO make the APSO advantageous in terms of optimization, with better capability to find solutions and convergences. The mathematical expression related to APSO is presented in (33)–(37). Here, the P is taken as the total population, with V as its velocity, m is varying from 1, 2, …, P, and it is the variation of P (particle). The $S^{(i+1)}$ and $V^{(k+1)}$ are population and velocity for the $(k+1)$th iteration, where the velocity and position for the former iteration are $V^{(k)}$ and $S^{(k)}$. For the $(k+1)$th iteration, the velocity and position will be updated using the expression given in (33) and (34) [28].

$$V^{(k+1)} = \rho[w^{(k)} \times V^{(k)} + c_1 \times r_1 \times \left(S^{personalbest} - S\right) + c_2 \times r_2 \times \left(\left(S^{globalbest}\right) - S\right)] \tag{33}$$

$$S^{(k+1)} = S^{(k)} + V^{(k+1)} \tag{34}$$

$$w^k = w_{\max} - (w_{\max} - w_{\min}) \frac{Itr^k}{Itr_{\max}} \tag{35}$$

$$\rho = \frac{2}{\left|2 - \psi - \sqrt{\psi^2 - 4\psi}\right|} \tag{36}$$

$$\psi = C^1 + C^2 = 4.1 \tag{37}$$

where, V, S, w, Itr, Itr_{max}, and k are defined as velocity, particle position, weight for inertia, iteration, maximum iteration, and respective kth iteration. The w_{min} = 0.9 and w_{max} = 0.4 are min and max weights, as given in [33]. The ρ = 0.729 is the constriction factor. Both C^1, C^2 = 2.05, and r_1, r_2 = random number between 0 and 1. The personal-best and global-best populations are denoted $S^{personalbest}$ and $S^{globalbest}$.

4.5. Grey Wolf Optimization (GWO) Technique

The GWO is proposed in 2014, as given in [19]. The GWO is a technique for optimization based on gray wolves' behavior and their hunting strategy. In a group, they obey a resilient leadership hierarchy of four levels of wolves, such as alpha (α), beta (β), delta (δ), and omega (ω) wolves headed by α level wolves. The α in level one is the authority to make decisions. The wolves in the β level usually help the leader. Wolves in level three are called δ wolves, and they are responsible for passing information to α, β wolves and controlling ω (last-level wolves). In the hierarchy of the grey wolves, α is considered as the most appropriate solution/result, whereas β and δ are the second and third most appropriate solution, respectively, and ω is the least appropriate solution of the population. Their hunting process comprises three different parts, such as searching, encircling (exploration), and attacking (exploitation) the prey.

- In GWO, the wolves' encircling process is mathematically expressed in Equations (38) and (39):

$$D = |C \times S_P(\mathrm{t}) - S(\mathrm{t})| \tag{38}$$

$$S(\mathrm{t}+1) = |S_P(\mathrm{t}) - A \times D| \tag{39}$$

where, A and C are the coefficient vectors, and they are calculated as follows:

$$A = 2 \times a \times r_1 - a \tag{40}$$

$$C = 2 \times r_2 \tag{41}$$

where S_p, S, t, a, and (r_1, r_2) are the victim/prey location, wolf location, current iteration, the linearly decaying value from 2 to 0, and a random number between [0, 1], respectively.

- In this algorithm, it is assumed that the hunting is executed by α, β, and δ because they have more expertise in searching for the prey location, whereas the ω just obey these wolves, as per their position. Hence, the adjustment of these leading wolves' positions are presented mathematically as follows:

$$\left\{ \begin{array}{c} D_\alpha = |C_1 \times S_\alpha - S| \\ D_\beta = |C_2 \times S_\beta - S| \\ D_\delta = |C_3 \times S_\delta - S| \end{array} \right\} \tag{42}$$

The values of S_α, S_β, and S_δ are the best three wolves in each iteration, respectively.

$$\left\{ \begin{array}{c} S_1 = |S_\alpha - A_1 \times D_\alpha| \\ S_2 = |S_\beta - A_2 \times D_\beta| \\ S_3 = |S_\delta - A_3 \times D_\delta| \end{array} \right\} \tag{43}$$

$$S_p(\mathrm{t}+1) = \frac{S_1 + S_2 + S_3}{3} \tag{44}$$

The (44) represents the new position of the prey as a mean of the best three wolves' position in the population. The grey wolves accomplish their hunting by attacking the prey. To attack, they must be close enough to the prey. The 'A' value lies between [−2a, 2a]. If the value of $|A| < 1$, they will attack the prey. Otherwise, the hunt will be abandoned to find a new better solution. This process will be repeated until the stopping criteria are met.

4.6. Grey Wolf-Particle Swarm Optimization (GWO-PSO) Technique

Though the PSO is better for the global optimum solution, it has the possibility to trap into the local optimum solution. In contrast, the GWO has the advantage of better exploration, exploitation, and convergence, which create less possibility for local optimum solution [19]. However, despite having these advantages, its ability to make the balance between exploration and exploitation is still somewhat dependent/limited on some of the mechanisms.

Therefore, to obtain the desired global optimum solution without being stuck in the local optimum solution, both the GWO and PSO are combined. Hence, in the proposed hybrid GWO-PSO technique [20–22], the GWO will be executed first, then it will give the best position alpha (S_α). After that, the execution of PSO takes place with S_α in place of $S^{personalbest}$ in order to determine the particle velocity. This process returns the updated/modified position back to the GWO. Hence, this process will be repeated until the stopping criteria are reached.

The flowchart for the concurrent optimal planning of DGs (P_{RDGs} and Q_{DSTAT}), with or without reconfiguration in IEEE 33 and 69-bus RDN using APSO and GWO-PSO, is illustrated in Figures 7 and 8, in which TS_1, to TS_5, are five tie-switches. The P_{RDG1}, P_{RDG2}, P_{RDG3} and Q_{DSTAT1}, Q_{DSTAT2}, Q_{DSTAT3} are three real power solar-DG and three reactive power DG, respectively. The Loc_1, Loc_2, and Loc_3 are the three locations, along with the respective DG capacity. All the tie-switches, P_{RDGs}, Q_{DSTAT}, and locations are considered as decision variables in the proposed algorithm.

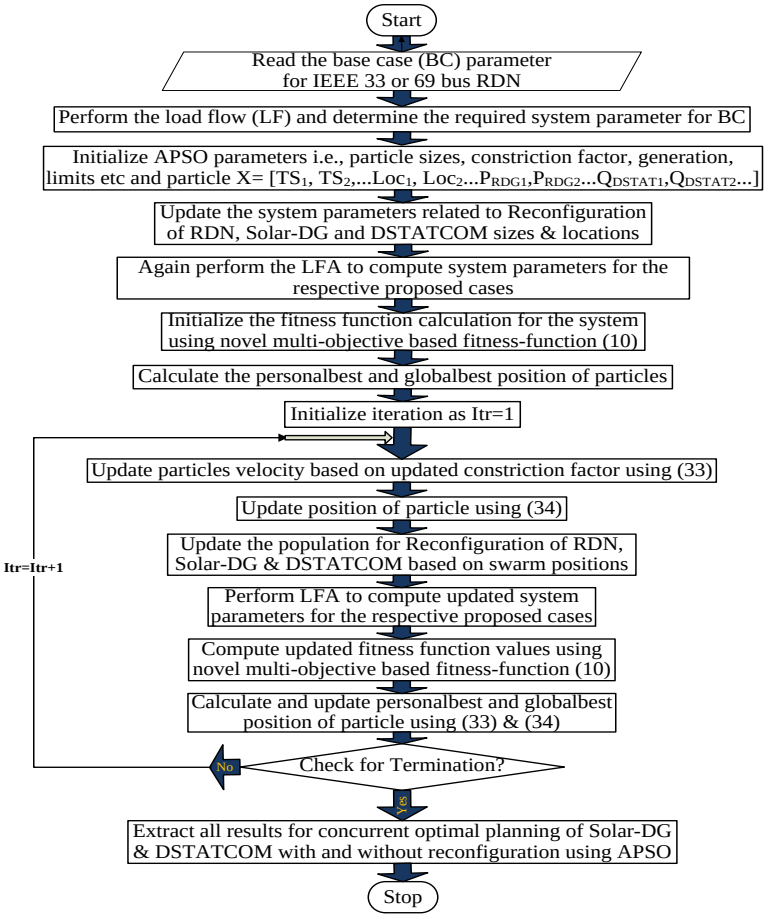

Figure 7. Flowchart for concurrent planning of multi Solar-DG and DSTATCOM in a reconfigured RDN using APSO technique.

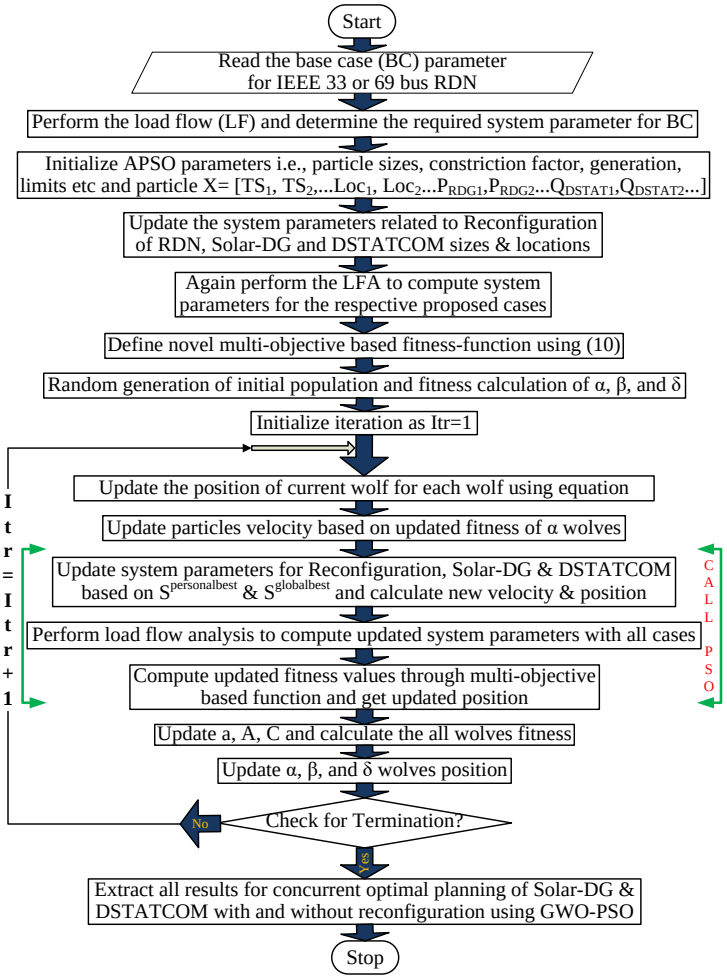

Figure 8. Flowchart for concurrent planning of multi Solar-DG and DSTATCOM in a reconfigured RDN using GWO-PSO technique.

5. Result and Discussion

In this paper, a novel multiple objective-based fitness-function (MO_F^F) is presented for the concurrent planning of multi-Solar-DG and DSTATCOM, with and without reconfiguration of RDN using the APSO and GWO-PSO techniques. Through the MATLAB 2018a platform, the said work has been carried out. The IEEE 33 and 69-bus RDN [37,38] are taken into consideration to analyze and validate the obtained results.

5.1. Analysis of 33-Bus Radial Distribution Network

The 33-bus RDN consists of 3.72 MW and 2.30 MVAr total active and reactive power loads, respectively. The data for the branch and load of the 33-bus IEEE test system [48] are presented in Figure 9 and the represented numbers are electric buses. The obtained outcomes for the PC-1 and PC-2 are illustrated in Tables 4–8 and Figures 10–18.

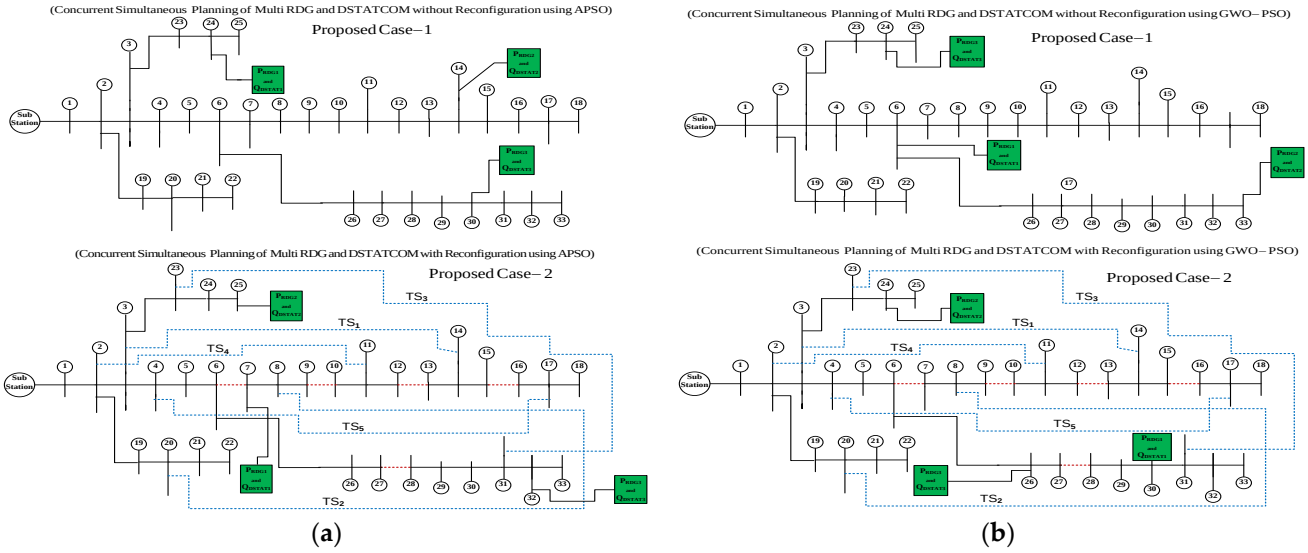

Figure 9. Proposed IEEE 33 bus RDN for both proposed cases; (**a**) APSO, (**b**) GWO-PSO.

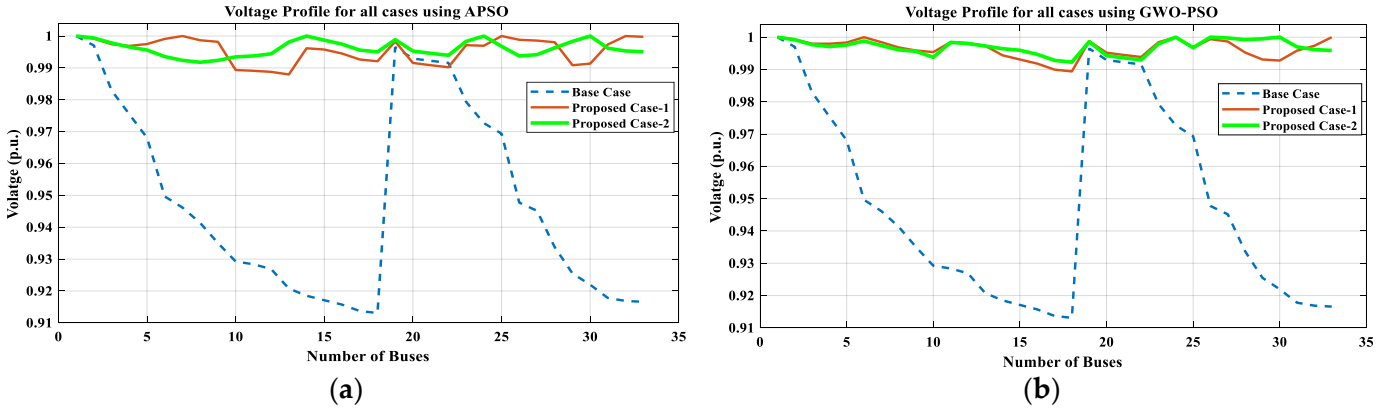

Figure 10. Voltage profile of 33-bus RDN for all cases; (**a**) APSO, (**b**) GWO-PSO.

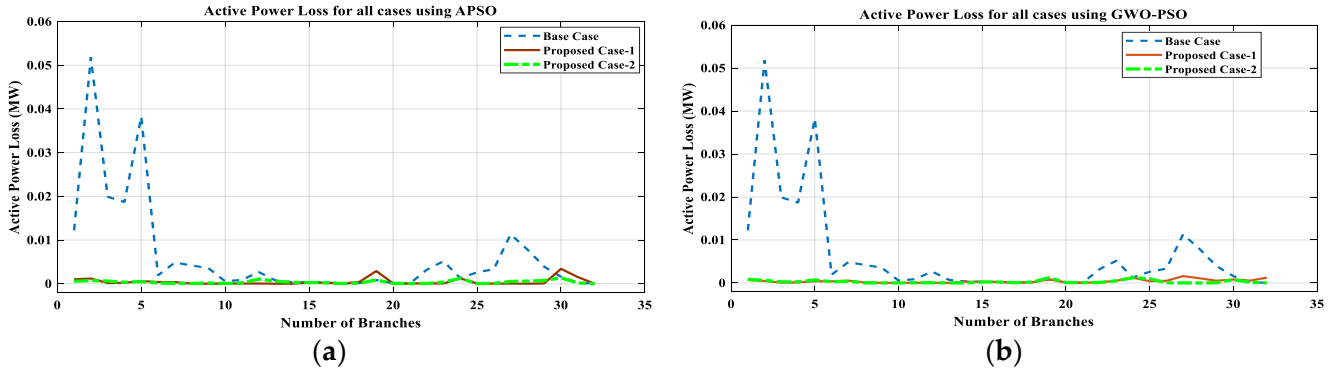

Figure 11. Real power loss for all cases of 33-bus RDN; (**a**) APSO, (**b**) GWO-PSO.

Table 4. Simultaneous optimal planning of DGs (in MW and MVAr) with and without reconfiguration of 33 bus RDN.

Cases	P & Q at Slack Bus (P_{SB_GEN}/ Q_{SB_GEN})	P_{RDG} (MW)/Bus No. (P_{RDG1}, P_{RDG2} & P_{RDG3})			Q_{DSTAT} (MVAr)/Bus No. (Q_{DSTAT}, Q_{DSTAT} & Q_{DSTAT})			TS_5, TS_4, TS_3, TS_2, & TS_1	Total P, Q and S Generation			Techniques
BC	3.92/2.44	—	—	—	—	—	—	—	3.92	2.44	4.6	—
PC-1	0.78/0.58	1.09/24	0.78/14	1.08/30	0.46/24	0.30/14	0.96/30	—	3.73	2.31	4.39	APSO
PC-2	0.98/0.89	1.04/7	0.87/25	0.83/32	0.28/7	0.32/25	0.83/32	0, 1, 0, 0 & 1	3.73	2.31	4.39	
PC-1	0.98/0.46	0.89/6	0.72/33	1.14/24	1.06/6	0.42/33	0.37/24	—	3.73	2.31	4.39	GWOPSO
PC-2	1.05/0.60	0.57/30	1.05/24	1.05/26	0.91/30	0.61/24	0.19/26	1, 1, 1, 1, & 1	3.73	2.31	4.39	

Table 5. The MO_F^F and its indices for IEEE 33 bus RDN.

Cases/Techniques	Fitness Function Indices										MO_F^F	
	IP_{Loss}		IQ_{Loss}		IV_D		$ISCLL_{Current}$		IR_S			
Techniques	APSO	GWOPSO	APSO	GWOPSO	APSO	GWOPSO	APSO	GWOPSO	APSO	GWOPSO	APSO	GWOPSO
PC-1	0.0763	0.0725	0.1051	0.1000	0.1019	0.1005	0.0796	0.0663	0.3756	0.3666	0.1095	0.0957
PC-2	0.0599	0.0500	0.0742	0.0624	0.0984	0.0979	0.0358	0.0069	0.3475	0.3265	0.1069	0.0909

Table 6. Losses, Short Circuit Level of Line Current ($SCLL_{Current}$), Deviation in Voltage (V_D) of the 33 bus RDN.

Cases/Techniques	Losses						$SCLL_{Current}$ (kA)		V_D (p.u.)	
	P_{Loss} (MW)		Q_{Loss} (MVAr)		S_{Loss} (MVA)					
Techniques	APSO	GWOPSO	APSO	GWOPSO	APSO	GWOPSO	APSO	GWOPSO	APSO	GWOPSO
BC	0.2027	0.2027	0.1351	0.1351	0.2435	0.2435	3.4118	3.4118	0.1869	0.1869
PC-1	0.0155	0.0147	0.0142	0.0135	0.0210	0.0199	0.2715	0.2263	0.1121	0.1106
PC-2	0.0121	0.0101	0.0100	0.0084	0.0156	0.0131	0.1220	0.0234	0.1082	0.1077

Table 7. Indices of Reliability of the IEEE 33 bus RDN.

Cases/ Techniques	Reliability Indices										R_S in %	
	SAIFI		SAIDI		CAIDI		ENS		RI SUM			
Techniques	**APSO**	**GWOPSO**	**APSO**	**GWOPSO**	**APSO**	**GWOPSO**	**APSO**	**GWOPSO**	**APSO**	**GWOPSO**	**APSO**	**GWOPSO**
BC	0.4869	0.4869	0.2921	0.2921	0.6	0.6	0.4869	0.4869	0.4665	0.4665	89.32	89.32
PC-1	0.0388	0.0323	0.0233	0.0194	0.6	0.6	0.0388	0.0323	0.1752	0.1710	96.12	96.77
PC-2	0.0174	0.0033	0.0104	0.0020	0.6	0.6	0.0205	0.0039	0.1621	0.1523	98.26	99.67

Table 8. Different cost of the IEEE 33 bus RDN.

Cases/Techniques	Fix Cost ($/Year)		Loss Cost ($/Year)		ENS Cost ($/Year)		Total Cost ($/Year)	
Techniques	**APSO**	**GWOPSO**	**APSO**	**GWOPSO**	**APSO**	**GWOPSO**	**APSO**	**GWOPSO**
BC	18,791.4171	18,791.4171	70,307.8843	70,307.884	8509.4763	8509.4763	97,608.7778	97,608.7778
PC-1	18,791.4171	18,791.4171	5363.7979	5100.3413	677.2700	564.5218	24,832.485	24,456.2802
PC-2	18,791.4171	18,791.4171	4209.1715	2515.1814	304.2684	1146.7351	23,304.857	22,453.3336

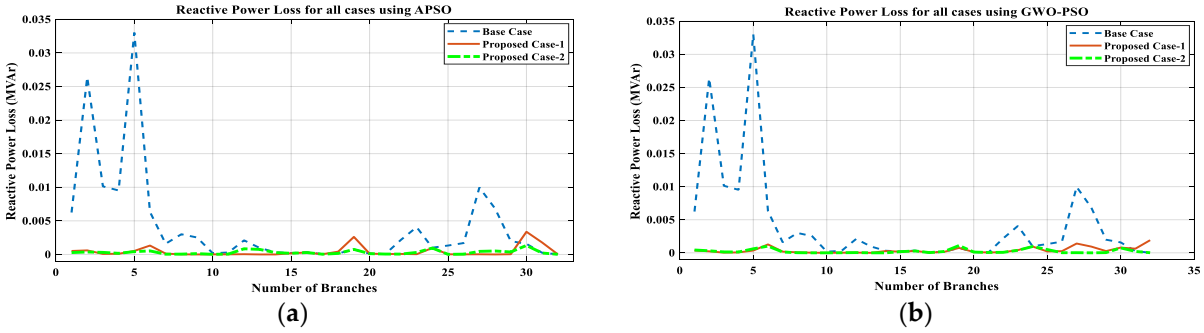

Figure 12. Reactive power loss for all cases of 33-bus RDN; (**a**) APSO, (**b**) GWO-PSO.

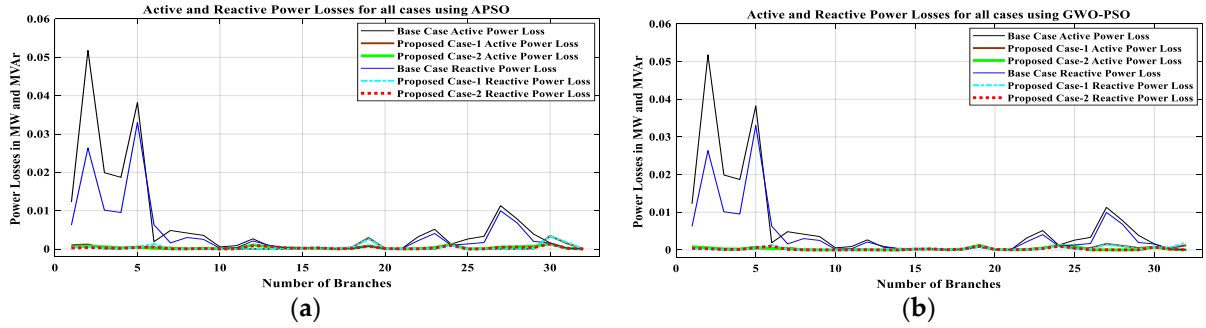

Figure 13. Cumulative representation of active and reactive power loss for all cases of 33-bus RDN; (**a**) APSO, (**b**) GWO-PSO.

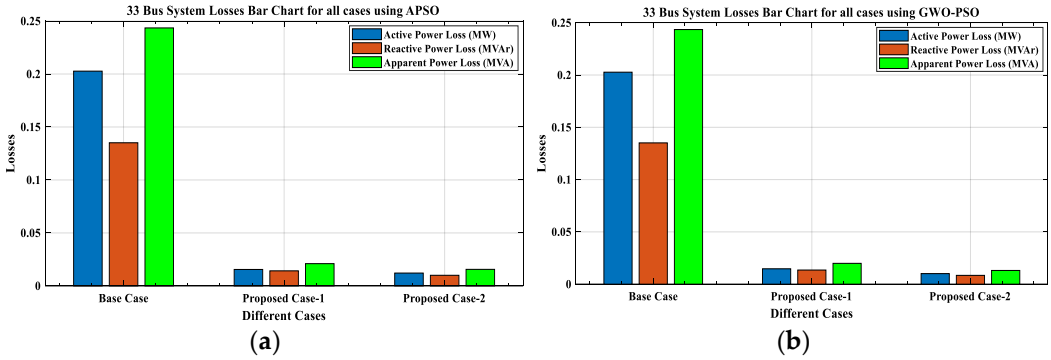

Figure 14. Cumulative bar representation of P_{Loss}, Q_{Loss}, and S_{Loss} for all cases of 33-bus RDN; (**a**) APSO, (**b**) GWO-PSO.

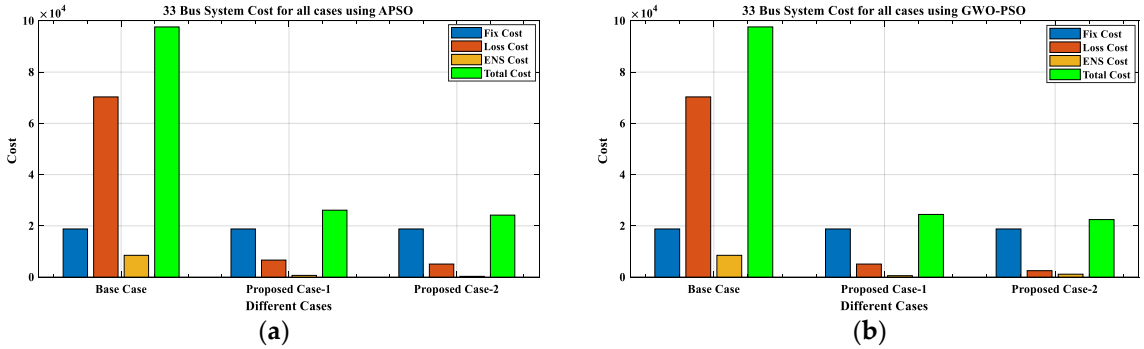

Figure 15. The fix, loss, and ENS cost for all the cases of 33-bus RDN; (**a**) APSO, (**b**) GWO-PSO.

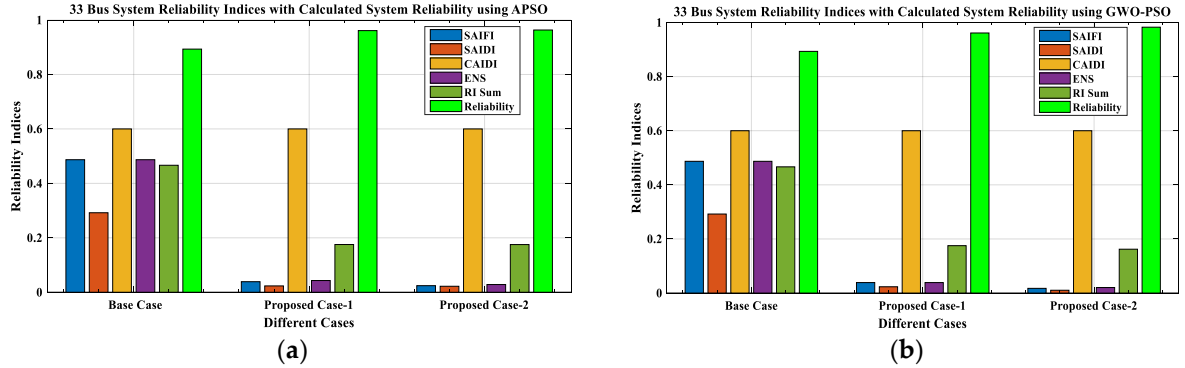

Figure 16. Reliability indices with system reliability of the 33-bus RDN; (**a**) APSO, (**b**) GWO-PSO.

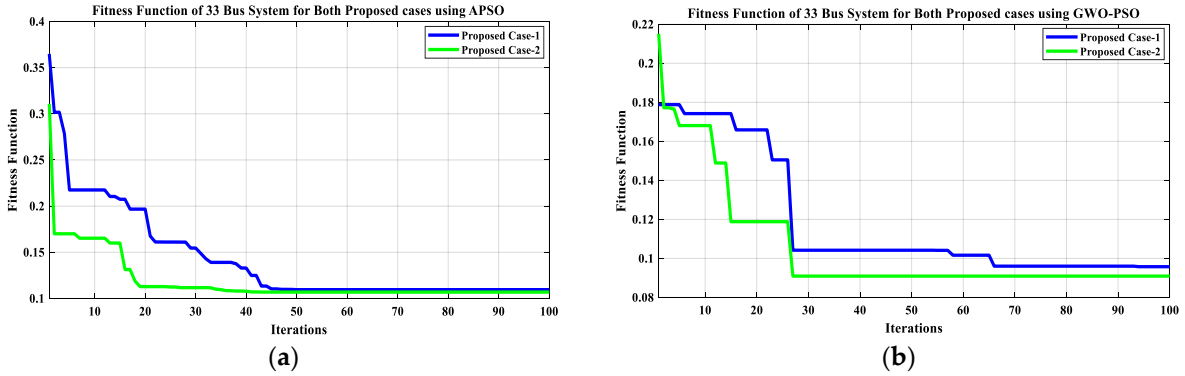

Figure 17. Proposed cases MO_F^F of the 33-bus RDN; (**a**) APSO, (**b**) GWO-PSO.

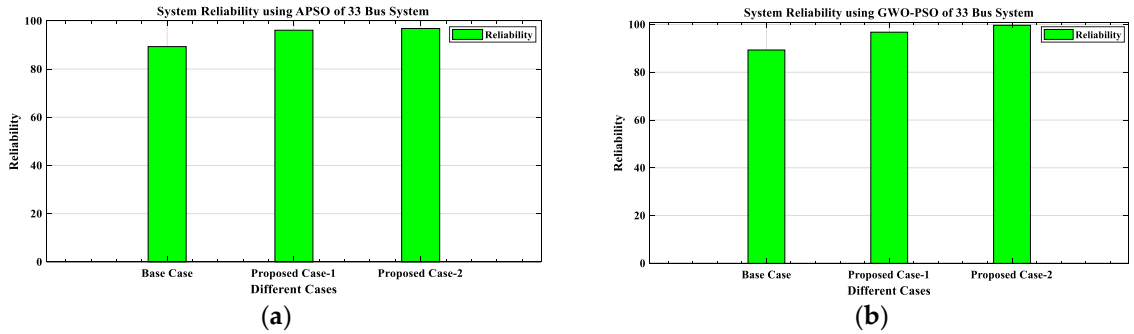

Figure 18. All proposed cases' percentage reliability of the 33-bus RDN; (**a**) APSO, (**b**) GWO-PSO.

The base case (BC) is considered as a case without DGs and reconfiguration. After the load flow analysis (LFA), the observed real power loss (P_{Loss}) is 0.2027 MW, and the reactive power loss (Q_{Loss}) is 0.1351 MVAr for the BC, as shown in Table 6. The maximum deviation in voltage (V_D) of the system is 0.1869 p.u. with respect to (w.r.t.) voltage reference, the short circuit level of line current ($SCLL_{Current}$) is 3.4118 kA, and the reliability is 89.32%, as seen from Tables 6 and 7.

5.1.1. The Proposed Case-1 (PC-1)

In PC-1 using APSO, 3 active and 3 reactive power DGs are optimally placed at bus numbers 24, 14, and 30 of the IEEE 33-bus RDN. The capacity of these DGs are 1.09 MW, 0.78 MW, 1.08 MW, and 0.46 MVAr, 0.30 MVAr, 0.96 MVAr, respectively, as shown in Table 4 and Figure 9a. After placing these DGs at optimal locations, the MO_F^F value is minimized to 0.1095, as given in Table 5. With this minimized MO_F^F, the system voltage profile is improved, with maximum (V_D) 0.1121 p.u. The P_{Loss} and Q_{Loss} is reduced to 0.0155 MW

and 0.0142 MVAr, respectively, as illustrated in Table 6 and Figures 10–14. Most importantly, the short circuit/fault tolerance capacity of the system is enhanced, as the $SCLL_{Current}$ is reduced by 92.04%, with improved system reliability of 96.12%, as shown in Tables 6 and 7. In this implementation, the fix cost is the same, with the value of USD 18,791.4171/year. However, the cost related to loss and ENS is reduced to USD 5363.7979/year and USD 677.2700/year from USD 70,307.8843/year and USD 8509.4763/year, respectively. Hence, there is a reduction in total cost, as it was USD 97,608.7778/year in the BC, and in PC-1, it is USD 24,832.485/year, as mentioned in Table 8 and Figure 15a.

Similarly, DGs are planned using the GWO-PSO technique to present a comparative analysis between both techniques, i.e., APSO and GWO-PSO. The optimal locations using GWO-PSO are at bus numbers 6, 33 and 24. The optimal sizes of DGs are 0.89 MW, 0.72 MW, 1.14 MW and 1.06 MVAr, 0.42 MVAr, 0.37 MVAr from real and reactive power perspective, as illustrated in Table 4 and Figure 9b. After placing these DGs at optimal locations, the MO_F^F value is minimized to 0.0957, as mentioned in Table 5. With this minimized MO_F^F, the system voltage profile is improved, with a maximum V_D of 0.1106 p.u. The P_{Loss} and Q_{Loss} are reduced to 0.0147 MW and 0.0135 MVAr, respectively, as illustrated in Table 6 and Figures 10–14. Most importantly, the short circuit/fault tolerance capacity of the system is enhanced, as the $SCLL_{Current}$ is reduced by 93.37%, with an improved system reliability of 96.77%, as shown in Tables 6 and 7. In this implementation, the fix cost is the same, with the value of USD 18,791.4171/year. However, the cost related to loss and ENS is reduced to USD 5100.3413/year and USD 564.5218/year from USD 70,307.8843/year and USD 8509.4763/year, respectively. Hence, the total cost is observed as USD 24,456.2802/year, which is less than the BC, as given in Table 8 and Figure 15b.

5.1.2. The Proposed Case-2 (PC-2)

In PC-2, using APSO, multiple DG planning with reconfiguration has been carried out without disturbing the system radiality. Three active and three reactive power DGs (P_{RDG} and Q_{DSTAT}) are optimally placed with reconfiguration at bus numbers 7, 25, and 32 of the IEEE 33-bus RDN. The capacities of all the optimal P_{RDG} and Q_{DSTAT} at these buses are 1.04 MW, 0.87 MW, 0.83 MW, and 0.83 MVAr, 0.28 MVAr, 0.32 MVAr, with TS_1 and TS_4 active tie-switches, as shown in Table 4 and Figure 9a. After placing these DGs at optimal locations, the MO_F^F value is minimized to 0.1069, as given in Table 5. With this minimized MO_F^F, the system voltage profile is improved, with a maximum V_D of 0.1082 p.u. The P_{Loss} and Q_{Loss} are reduced to 0.0121 MW and 0.0100 MVAr with 0.0156 MVA as S_{Loss}, respectively, as illustrated in Table 6, Figures 10a, 11a, 12a, 13a and 14a. Most importantly, the short circuit/fault tolerance capacity of the system is enhanced, as the $SCLL_{Current}$ is reduced by 96.42%, with an improved system reliability of 98.26%, as shown in Tables 6 and 7. In PC-2, using APSO, the fix cost value is still fixed, with the value of USD 18,791.4171/year. At the same time, the cost related to loss and ENS is reduced to USD 4209.1715/year and USD 304.2684/year from USD 70,307.8843/year and USD 8509.4763/year, respectively. Hence, there is a reduction in total cost, as it was USD 97,608.7778/year in the BC, but in PC-2, its value reduced to USD 23,304.857/year, as illustrated in Table 8 and Figure 15a.

Similarly, in PC-2, using the GWO-PSO technique, DGs are planned with reconfiguration without disturbing the system radiality to present a comparative analysis between both the techniques, i.e., APSO and GWO-PSO. The optimal locations using GWO-PSO are at bus number 30, 24, and 26. The capacities of P_{RDG} in MW and Q_{DSTAT} in MVAr at these buses are 0.57 1.05, 1.05 and 0.91, 0.61, 0.19, with all TS_1 to TS_5 active tie-switches, as illustrated in Table 4 and Figure 9b. After placing these DGs at optimal locations, the MO_F^F value is minimized to 0.0909, as given in Table 5. With this minimized MO_F^F, the system voltage profile is improved, with a maximum V_D of 0.1077 p.u. The P_{Loss} and Q_{Loss} are reduced to 0.0101 MW and 0.0084 MVAr with 0.0131 MVA as S_{Loss}, respectively, as illustrated in Table 6, Figures 10b, 11b, 12b, 13b and 14b. Most importantly, the short circuit/fault tolerance capacity of the system is enhanced, as the $SCLL_{Current}$ is reduced by 99.31%, with an improved system reliability of 99.67% w.r.t. BC, as shown in Tables 6 and 7. In PC-2, us-

ing GWO-PSO, the cost related to loss and ENS is reduced to USD 2515.1814/year and USD 1146.7351/year from USD 70,307.8843/year and USD 8509.4763/year, respectively, with no change in fix cost. Hence, there is a reduction in total cost, as it was USD 97,608.7778/year in the BC, but in PC-2, it is USD 22,453.3336/year, as mentioned in Table 8 and Figure 15b.

After placing the DGs at optimal locations with reconfiguration in IEEE 33-bus RDN, it has been observed that the total real and reactive power drawn by the system (which includes P_{SB_GEN}, Q_{SB_GEN} and P_{RDG}, Q_{DSTAT}) is reduced to 3.73 MW and 2.31 MVAr, respectively, in which the total real and reactive power generation is 4.85% and 5.33% less than the BC. Hence, with this novel implementation (PC-2) using APSO and GWO-PSO, the P_{Loss} is reduced by 94.03% and 95.02%, Q_{Loss} is reduced by 92.59% and 93.78%, and V_D is also decreased by 42.11% and 42.37%, respectively, as shown in Table 6 and Figures 10–14. The $SCLL_{Current}$ is reduced by 96.42% and 99.31% using APSO and GWO-PSO separately. Consequently, the reliability is increased up to 98.26% and 99.67%, as it was 89.32% in BC, as given Table 7 and Figure 18b.

From the comparative analysis between APSO and GWO-PSO, it can be concluded that the outcomes of GWO-PSO are superior to the APSO. Finally, the detailed analysis of the results indicates that the concurrent optimal planning of multi-Renewable Solar-DG and DSTATCOM in a Reconfigured IEEE 33-bus RDN using the APSO and GWO-PSO techniques is an effective approach to minimize the MO_F^F, and its minimized outcome is illustrated in Table 5, as well as in Figure 17 as a graphical representation.

5.1.2.1. 69-Bus Radial Distribution Network

The 69-bus RDN consists of 3.80 MW and 2.69 MVAr total active and reactive power loads, respectively. The data for the branch and load of the 69-bus IEEE test system [48,51] are presented in Figure 19 and the given numbers are representing the electric buses. The obtained outcomes for the PC-1 and PC-2 are illustrated in Tables 9–13 and Figures 20–28.

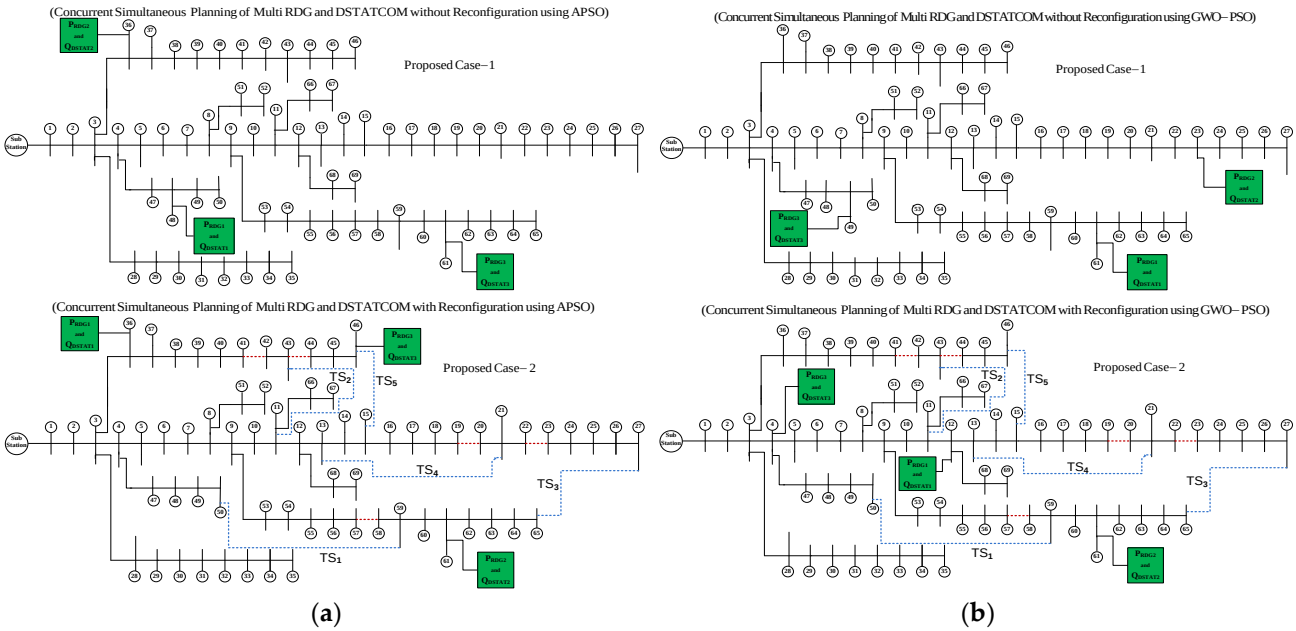

Figure 19. Proposed IEEE 69-bus RDN for both proposed cases; (**a**) APSO, (**b**) GWO-PSO.

Table 9. Simultaneous optimal planning of DGs (in MW and MVAr) with and without reconfiguration of 69-bus RDN.

Cases	P & Q at Slack Bus (P_{SB_GEN}/Q_{SB_GEN})	P_{RDG} (MW)/Bus No. (P_{RDG1}, P_{RDG2} & P_{RDG3})			Q_{DSTAT} (MVAr)/Bus No. (Q_{DSTAT}, Q_{DSTAT} & Q_{DSTAT})			TS_5, TS_4, TS_3, TS_2, & TS_1	Total P, Q and S Generation			Techniques
BC	4.03/2.80	—	—	—	—	—	—	—	4.03	2.8	4.9	—
PC-1	−2.52/1.73	2.00/48	2.60/36	1.75/61	0.16/48	−0.71/36	1.53/61	—	3.83	2.71	4.69	APSO
PC-2	−2.24/1.7	3.60/36	1.95/61	0.50/46	−1.18/36	1.55/61	0.64/46	1, 0, 1, 1, & 1	3.81	2.7	4.67	
PC-1	−0.06/1.10	1.80/61	0.51/23	1.56/49	1.12/61	0.22/23	0.26/49	—	3.81	2.7	4.67	GWOPSO
PC-2	0.27/0.02	0.89/12	2.39/61	0.27/4	0.41/12	1.15/61	1.11/4	1, 1, 1, 1, & 1	3.81	2.7	4.67	

Table 10. The MO_F^F and its indices for IEEE 69-bus RDN.

Cases/Techniques	Fitness Function Indices										MO_F^F	
	IP_{Loss}		IQ_{Loss}		IV_D		$ISCLL_{Current}$		IR_S			
Techniques	**APSO**	**GWOPSO**	**APSO**	**GWOPSO**	**APSO**	**GWOPSO**	**APSO**	**GWOPSO**	**APSO**	**GWOPSO**	**APSO**	**GWOPSO**
PC-1	0.1137	0.0647	0.1575	0.1070	0.1157	0.1042	0.0288	0.0167	0.2287	0.2101	0.1011	0.0757
PC-2	0.0471	0.0424	0.0689	0.0605	0.0958	0.0918	0.0001	0.0053	0.2059	0.1747	0.0725	0.0656

Table 11. Losses, Short Circuit Level of Line Current ($SCLL_{Current}$), Deviation in Voltage (V_D) of the 69-bus RDN.

Cases/Techniques	Losses						$SCLL_{Current}$ (kA)		V_D (p.u.)	
	P_{Loss} (MW)		Q_{Loss} (MVAr)		S_{Loss} (MVA)					
Techniques	**APSO**	**GWOPSO**	**APSO**	**GWOPSO**	**APSO**	**GWOPSO**	**APSO**	**GWOPSO**	**APSO**	**GWOPSO**
BC	0.225	0.225	0.1022	0.1022	0.2471	0.2471	6.6534	6.6534	0.1908	0.1908
PC-1	0.0256	0.0146	0.0161	0.0109	0.0302	0.0182	0.1914	0.1757	0.1273	0.1146
PC-2	0.0106	0.0087	0.0070	0.0062	0.0127	0.0107	0.0006	0.0352	0.1053	0.1015

Table 12. Indices of Reliability of the IEEE 69-bus RDN.

Cases/Techniques	Reliability Indices										R_S in %	
	SAIFI		SAIDI		CAIDI		ENS		RI SUM			
Techniques	**APSO**	**GWOPSO**	**APSO**	**GWOPSO**	**APSO**	**GWOPSO**	**APSO**	**GWOPSO**	**APSO**	**GWOPSO**	**APSO**	**GWOPSO**
BC	0.8902	0.8902	0.5341	0.5341	0.6	0.6	0.8902	0.8902	0.7287	0.7287	84.36	84.36
PC-1	0.0256	0.0182	0.0154	0.0069	0.6	0.6	0.0256	0.00246	0.1666	0.1624	96.42	97.18
PC-2	0.0001	0.0047	0.0001	0.0028	0.6	0.6	0.0001	0.0047	0.1501	0.1531	96.78	96.72

Table 13. The fix, loss, and ENS cost for all the cases of IEEE 69-bus RDN; (a) APSO, (b) GWO-PSO.

Cases/Techniques	Fix Cost ($/Year)		Loss Cost ($/Year)		ENS Cost ($/Year)		Total Cost ($/Year)	
Techniques	**APSO**	**GWOPSO**	**APSO**	**GWOPSO**	**APSO**	**GWOPSO**	**APSO**	**GWOPSO**
BC	18,230.327	18,230.327	78,051.832	78,051.832	16,594.715	16,594.715	11,2876.87	112,876.87
PC-1	18,230.327	18,230.327	8873.0903	5048.5566	477.3242	87.6699	27,580.742	23,366.5538
PC-2	18,230.327	18,230.327	3677.7492	3018.6946	1.5902656	173.1570	21,926.545	21,422.1786

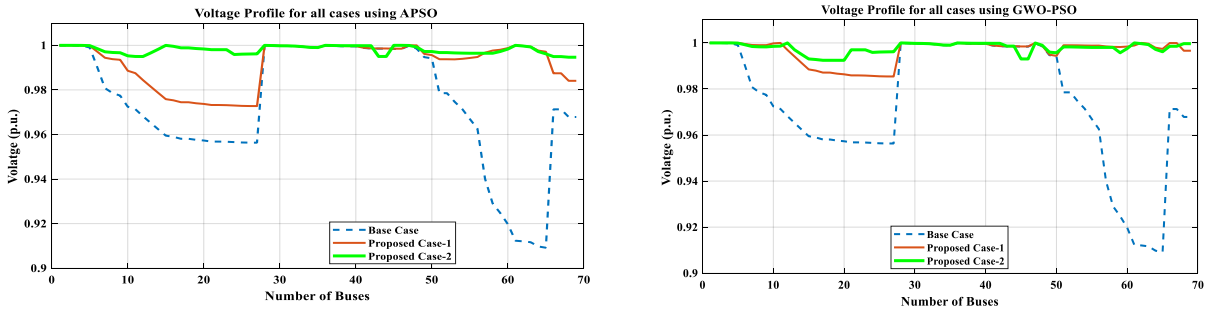

Figure 20. Voltage profile of 69-bus RDN for all cases; (**a**) APSO, (**b**) GWO.

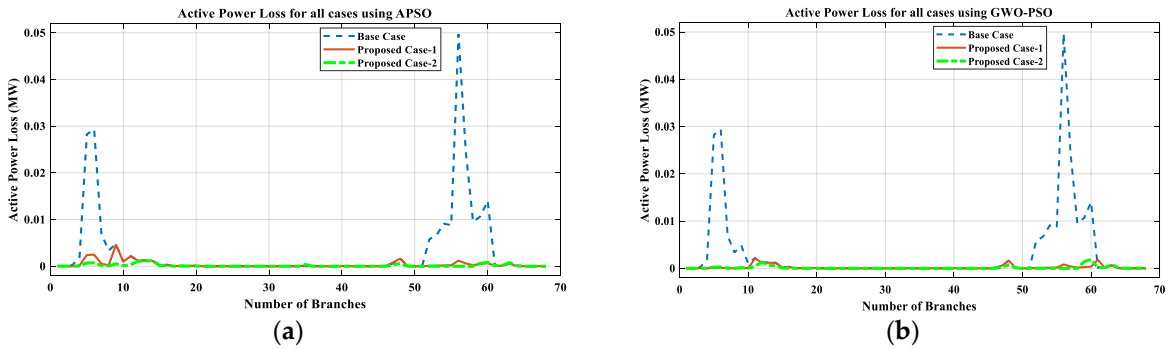

Figure 21. Real power loss for all cases of 69-bus RDN; (**a**) APSO, (**b**) GWO-PSO.

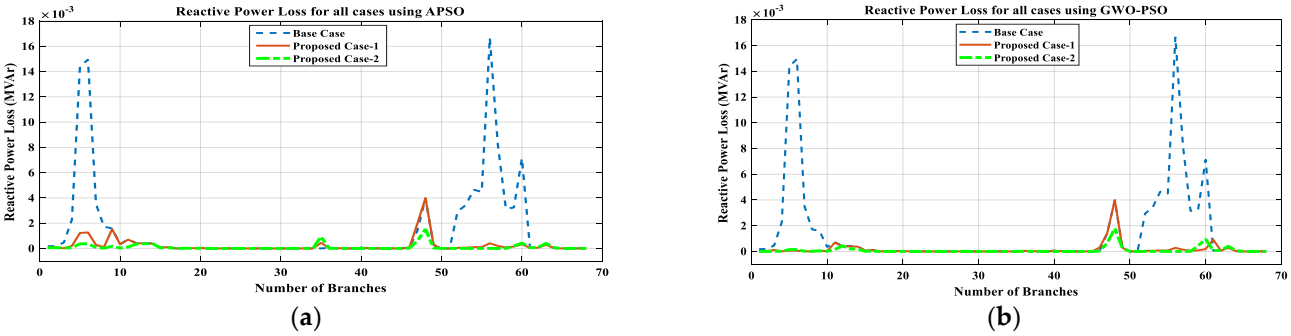

Figure 22. Reactive power loss for all cases of 69-bus RDN; (**a**) APSO, (**b**) GWO-PSO.

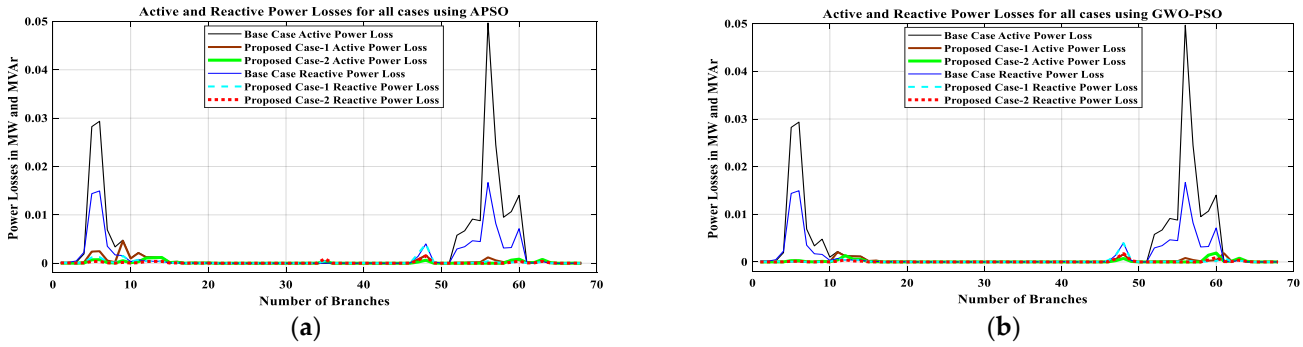

Figure 23. Cumulative representation of active and reactive power loss for all cases of 69-bus RDN; (**a**) APSO, (**b**) GWO-PSO.

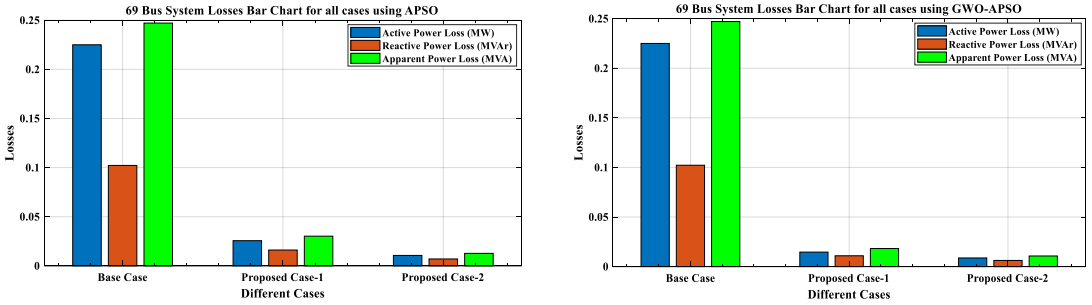

Figure 24. Cumulative bar representation of P_{Loss}, Q_{Loss}, and S_{Loss} for all cases of 69-bus RDN; (**a**) APSO, (**b**) GWO-PSO.

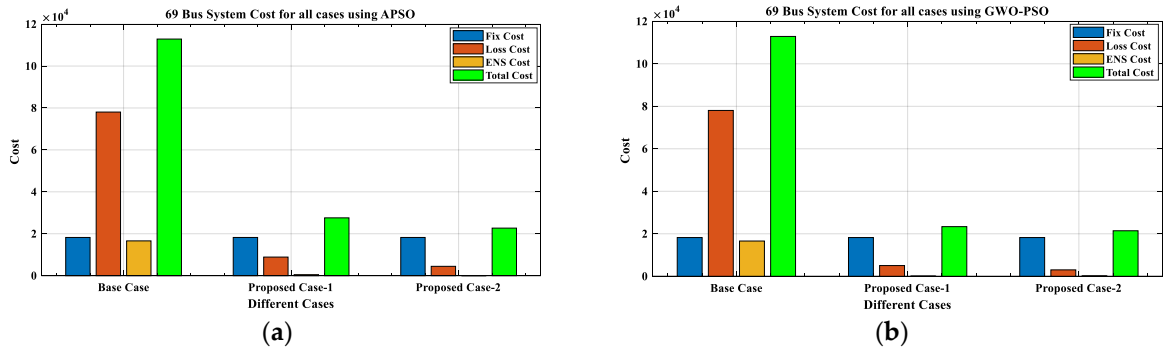

Figure 25. Cost for all cases of the 69-bus RDN; (**a**) APSO, (**b**) GWO-PSO.

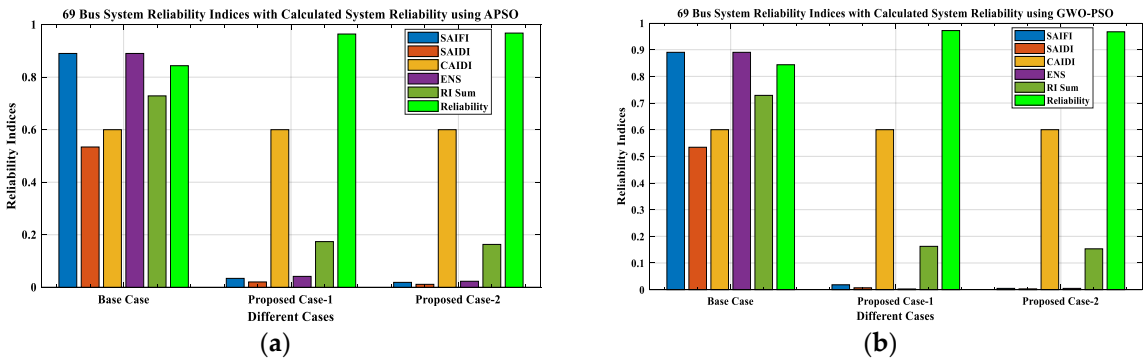

Figure 26. Reliability indices with system reliability of the 69-bus RDN; (**a**) APSO, (**b**) GWO-PSO.

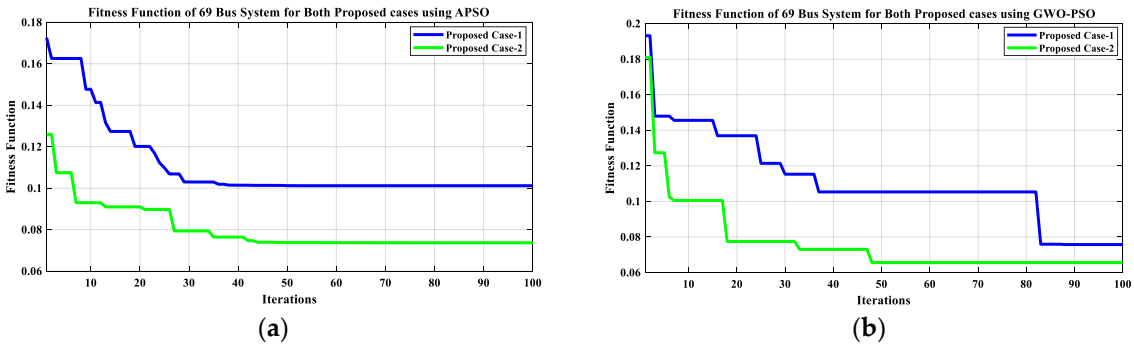

Figure 27. Proposed cases MO_F^F of the 69-bus RDN; (**a**) APSO, (**b**) GWO-PSO.

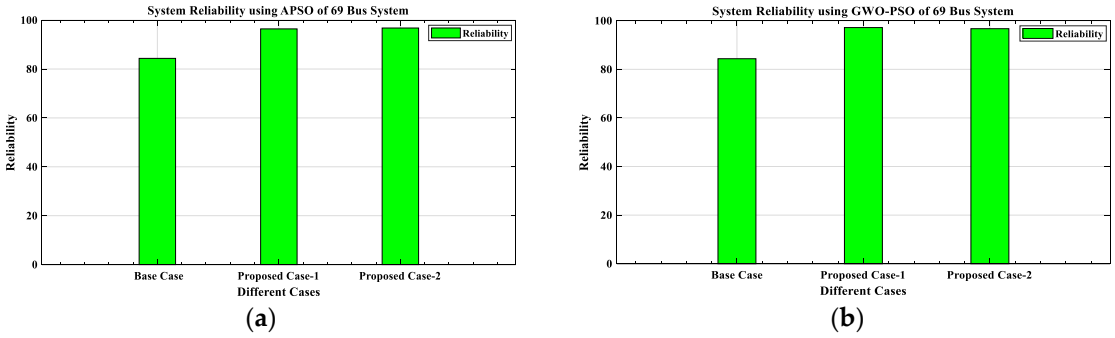

Figure 28. All proposed cases percentage reliability of the 69-bus RDN; (**a**) APSO, (**b**) GWO-PSO.

The base case (BC) is considered as a case without DGs and reconfiguration. After the LFA, the observed real power loss (P_{Loss}) is 0.225 MW, and the reactive power loss (Q_{Loss}) is 0.1022 MVAr for the BC, as shown in Table 6. The maximum deviation in voltage (V_D) of the system is 0.1908 p.u. with respect to (w.r.t.) voltage reference, the short circuit level of line current ($SCLL_{Current}$) is 6.6534 kA, and the reliability is 84.36%, as shown in Tables 10 and 11.

5.1.2.2. The Proposed Case-1 (PC-1)

In PC-1, using APSO, three active and three reactive power DGs are optimally placed at bus numbers 48, 36, and 61 of the IEEE 69-bus RDN. The capacity of these DGs are 2 MW, 2.6 MW, 1.75 MW, and 0.16 MVAr, −0.71 MVAr, 1.53 MVAr, respectively, as shown in Table 9 and Figure 19a. After placing these DGs at optimal locations, the MO_F^F value is minimized to 0.1017, as given in Table 10. With this minimized MO_F^F, the system voltage profile is improved, with a maximum V_D of 0.1273 p.u. The P_{Loss} and Q_{Loss} are reduced to 0.0256 MW and 0.0161 MVAr, respectively, as illustrated in Table 11 and Figures 20a, 21a, 22a, 23a and 24a. Most importantly, the short circuit/fault tolerance capacity of the system is enhanced, as the $SCLL_{Current}$ is reduced by 97.12%, with an improved system reliability of 96.42%, as shown in Tables 11 and 12 and Figure 28a. In this implementation, the fix cost is the same, with a value of USD 18,230.327/year. However, the cost related to loss and ENS is reduced to USD 8873.0903/year and USD 477.3242/year from USD 78,051.832/year and USD 16,594.715/year, respectively. Hence, there is a reduction in total cost, as it was USD 112,876.87/year in the BC, and in PC-1, it is USD 27,580.742/year, as mentioned in Table 13 and Figure 25a.

Similarly, DGs are planned using the GWO-PSO technique to present a comparative analysis between both techniques, i.e., APSO and GWO-PSO. The optimal locations using GWO-PSO are at bus numbers 61, 23, and 49. The optimal sizes of DGs are of 1.80 MW, 0.51 MW, 1.56 MW and 1.12 MVAr, 0.22 MVAr 0.26 MVAr from the real and reactive power perspective, as illustrated in Table 9 and Figure 19b. After placing these DGs at optimal locations, the MO_F^F value is minimized to 0.0757, as mentioned in Table 5. With this minimized MO_F^F, the system voltage profile is improved, with a maximum V_D of 0.1146 p.u. The P_{Loss} and Q_{Loss} are reduced to 0.0146 MW and 0.0109 MVAr, respectively, as illustrated in Table 11, Figures 20b, 21b, 22b, 23b and 24b. Most importantly, the short circuit/fault tolerance capacity of the system is enhanced, as the $SCLL_{Current}$ is reduced by 97.36%, with improved system reliability of 96.78%, as shown in Tables 11 and 12 and Figure 28b. In this implementation, the fix cost is the same, with the value of USD 18,230.327/year. However, the cost related to loss and ENS is reduced to USD 5048.5566/year and USD 87.6699/year from USD 78,051.832/year and USD 16,594.715/year, respectively. Hence, the total cost observed is USD 23,366.5538/year, which is less than the BC, as given in Table 13 and Figure 25b.

5.1.2.3. The Proposed Case-2 (PC-2)

In PC-2, using APSO, multiple DG planning with reconfiguration has been carried out without disturbing the system radiality. Three active and three reactive power DGs (P_{RDG} and Q_{DSTAT}) are optimally placed with reconfiguration at bus numbers 36, 61, and 46 of the IEEE 69 bus RDN. The capacities of all optimal P_{RDG} and Q_{DSTAT} at these buses are 3.60 MW, 1.95 MW, 0.50 MW, and −1.18 MVAr, 1.55 MVAr, 0.641 MVAr, with TS_1, TS_2, TS_3, and TS_5 active tie-switches, as shown in Table 9 and Figure 19b. After placing these DGs at optimal locations, the MO_F^F value is minimized to 0.0725, as given in Table 10. With this minimized MO_F^F, the system voltage profile is improved, with a maximum V_D of 0.1053 p.u. The P_{Loss} and Q_{Loss} are reduced to 0.0106 MW and 0.0070 MVAr with 0.0127 MVA as S_{Loss}, respectively, as illustrated in Table 11 and Figures 20–24. Most importantly, the short circuit/fault tolerance capacity of the system is enhanced, as the $SCLL_{Current}$ is reduced by 99.99%, with improved system reliability of 96.78%, as shown in Tables 11 and 12 and Figure 28a. In PC-2, using APSO, the fix cost value is still fixed, with the value of USD 18,230.327/year. At the same time, the cost related to loss and ENS is reduced to USD 3677.7492/year and USD 1.5903/year from USD 78,051.832/year and USD 16,594.715/year, respectively. Hence, there is a reduction in total cost, as it was USD 112,876.87/year in the BC, but in PC-2, its value reduced to USD 21,926.545/year, as illustrated in Table 13 and Figure 25a.

Similarly, in PC-2, using the GWO-PSO technique, DGs are planned with reconfiguration without disturbing the system radiality to present a comparative analysis between both the techniques, i.e., APSO and GWO-PSO. The optimal locations using GWO-PSO are at bus number 12, 61, and 4. The capacities of P_{RDG} in MW and Q_{DSTAT} in MVAr at these buses are 0.89, 2.39, 0.27, and 0.41, 1.15, 1.11, with all TS_1 to TS_5 active tie-switches, as illustrated in Table 9 and Figure 19b. After placing these DGs at optimal locations, the MO_F^F value is minimized to 0.0656, as given in Table 10. With this minimized MO_F^F, the system voltage profile is improved, with a maximum V_D of 0.1015 p.u. The P_{Loss} and Q_{Loss} is reduced to 0.0087 MW and 0.0062 MVAr with 0.0107 MVA as S_{Loss}, respectively, as illustrated in Table 11 and Figures 20–24. Most importantly, the short circuit/fault tolerance capacity of the system is enhanced, as the $SCLL_{Current}$ is reduced by 99.47%, with an improved system reliability of 96.72% w.r.t. BC, as shown in Tables 11 and 12 and Figure 28b. In PC-2, using GWO-PSO, the cost related to loss and ENS is reduced to USD 3018.6946/year and USD 173.1570/year from USD 78,051.832/year and USD 16,594.715/year, respectively, with no change in fix cost. Hence, there is a reduction in total cost, as it was USD 112,876.87/year in the BC, but in PC-2, it is USD 21,422.1786/year, as mentioned in Table 13 and Figure 25. The reliability indices with system reliability of the 69-bus are shown in Figure 26. The proposed cases' MO_F^F of the 69-bus are presented in Figure 27.

After placing the DGs at optimal locations with reconfiguration in IEEE 69-bus RDN, it has been observed that the total real and reactive power drawn by the system (which includes P_{SB_GEN}, Q_{SB_GEN} and P_{RDG}, Q_{DSTAT}) are reduced to 3.81 MW and 2.70 MVAr, respectively, in which the total real and reactive power generation is 5.46% and 3.57% less than the BC. Hence, with this novel implementation, (PC-2) using APSO and GWO-PSO, the P_{Loss} is reduced by 95.29% and 96.14%, Q_{Loss} is reduced by 93.15% and 93.94%, and V_D is also decreased by 44.81% and 46.80%, respectively, as shown in Table 11 and Figures 20b, 21b, 22b, 23b and 24b. The $SCLL_{Current}$ is reduced by 99.99% and 99.47% using APSO and GWO-PSO separately. Consequently, the reliability is increased up to 96.78% and 96.72%, as it was 84.36% in BC, as given in Table 12 and Figure 28b.

From the comparative analysis between APSO and GWO-PSO, it can be concluded that the outcomes of GWO-PSO are superior to APSO. Finally, the detailed analysis of results indicates that the concurrent optimal planning of multi-Renewable Solar-DG and DSTATCOM in a Reconfigured IEEE 69-bus RDN using the APSO and GWO-PSO techniques is an effective approach to minimize the MO_F^F, and its minimized outcome is illustrated in Table 10, as well as in Figure 27 as a graphical representation.

In Table 14, a comparison of the proposed work of this paper and other excerpted works from the literature [52–54] is presented. Hence, from this comparative analysis, it is found that the proposed work's outcomes tabulated in Tables 6 and 11 are much better than those in the existing work.

Table 14. The comparative analysis of the proposed work with existing work on 33- and 69-bus RDN.

Proposed/ Existing Work	Technique for Optimization	Magnitude		% Reduction	
		P_{Loss} (kW)	V_D (p.u.)	P_{Loss}	V_D
For IEEE 33 Bus Distribution Network					
Vempalle, et al. [52]	PSO and Dragonfly Algorithm	63.50	0.1522	68.67	18.57
Muhammad, et al. [53]	Water Cycle Algorithm	51.74	—	74.47	—
	Harmony Search Algorithm	96.83	—	51.99	—
	Fireworks Algorithm	68.27	—	66.32	—
	Cuckoo Search Algorithm	54.23	—	73.25	—
	Uniform voltage distribution based Constructive Algorithm	57.28	—	71.74	—
Rahim, et al. [54]	Firefly Algorithm (FA)	72.36	0.1249	64.30	33.17
	Evolutionary Programming Algorithm	73.34	0.1268	63.82	32.15
Work Proposed	Adaptive PSO	12.10	0.1082	94.03	42.11
	GWO-PSO	10.10	0.1077	95.02	42.38
For IEEE 69 Bus Distribution Network					
Oda, et al. [1]	ALO	71.71	—	68.13	—
	MALO	69.43	—	69.14	—
Vempalle, et al. [52]	PSO and Dragonfly Algorithm	39.20	0.1375	82.6	27.93
Muhammad, et al. [53]	Water Cycle Algorithm	35.04	—	84.42	—
	Harmony Search Algorithm	59.44	—	73.58	—
	Fireworks Algorithm	39.57	—	82.41	—
	Cuckoo Search Algorithm	36.90	—	83.6	—
	Uniform voltage distribution based Constructive Algorithm	37.00	—	83.56	—
Rahim, et al. [54]	Firefly Algorithm (FA)	39.54	0.1184	82.47	37.94
	Evolutionary Programming Algorithm	40.34	0.1184	82.07	37.94
Work Proposed	Adaptive PSO	10.60	0.1053	95.29	44.81
	GWO-PSO	8.70	0.1015	96.14	46.80

6. Conclusions

The concurrent optimal planning of multiple Solar-DG and DSTATCOM in IEEE 33- and 69-bus reconfigured RDN has been done using APSO and GWO-PSO, based on a proposed novel multiple objective-based fitness-function (MO_F^F). This MO_F^F consists of different system indices, such as loss in real power (P_{Loss}), loss in reactive power (Q_{Loss}), deviation in voltage (V_D), short circuit level of line current ($SCLL_{Current}$), and system reliability (R_S). The economic perspective of the system has also been considered, based on the various costs, such as the fix, loss, and Energy Not Supplied (ENS) cost. A detailed comparative analysis of obtained results using the APSO and GWO-PSO techniques has

been presented for both IEEE 33 and 69-bus RDN. Thereafter, it has been observed that between both proposed cases, i.e., PC-1 and PC-2, PC-2 using GWO-PSO performs better.

This analysis using APSO and GWO-PSO in PC-2, as compared to PC-1, for IEEE 33-bus RDN shows an improved voltage profile, with a maximum V_D of 0.1082 p.u. and 0.1077 p.u., respectively. It was 0.1869 p.u. in the base case (BC), as demonstrated in Table 6 and Figure 10. A significant reduction is noticed in the P_{Loss} with 0.0121 MW and 0.0101 MW using APSO and GWO-PSO, respectively. The Q_{Loss} is decreased to 0.0100 MVAr and 0.0084 MVAr, as given in Table 6 and Figures 11–14. Consequently, the $SCLL_{Current}$ is reduced by 96.42% and 99.31%, which is why the short circuit/fault tolerance capacity of the system is enhanced, which can be seen in Table 6. Hence, the R_S in PC-2 for IEEE 33-bus RDN are enhanced by 98.26% and 99.67%, as compared with BC data, as illustrated in Table 7 and Figure 18. From the economic perspective, savings in loss and ENS costs are noticed. Hence, the total cost is reduced to USD 23,304.857/year and USD 22,453.3336/year using APSO and GWO-PSO, respectively, for IEEE 33-bus RDN, as presented in Table 8 and Figure 15.

Similarly, the analysis for IEEE 69-bus RDN using APSO and GWO-PSO in PC-2 shows an improved voltage profile, with a maximum V_D of 0.1053 p.u. and 0.1015 p.u., respectively. It was 0.1908 p.u. in the base case (BC), as demonstrated in Table 9 and Figure 20. A significant reduction is noticed in the P_{Loss} with 0.0106 MW and 0.0087 MW using APSO and GWO-PSO, respectively. The Q_{Loss} decreased to 0.0070 MVAr and 0.0062 MVAr, as given in Table 9 and Figures 21–24. Consequently, the $SCLL_{Current}$ decreased by 96.99% and 99.47%, which is why the short circuit/fault tolerance capacity of the system is enhanced, which can be seen in Table 9. Hence, the R_S in PC-2 for IEEE 33-bus RDN is enhanced by 96.78% and 96.72%, as compared with BC data, as illustrated in Table 12 and Figure 28. From the economic perspective, savings in loss and ENS costs are noticed. Hence, the total cost is reduced to USD 21,926.545/year and USD 21,422.1786/year using APSO and GWO-PSO, respectively, for IEEE 33-bus RDN, as presented in Table 13 and Figure 25.

After analyzing the results of the proposed work, a comparison between the proposed work results with other existing works is presented in Table 14. From this comparative analysis, it is found that the proposed work's outcomes, as tabulated in Tables 6 and 11, are much better than the existing works. While commenting on the superiority of results between APSO and GWO-PSO, the result obtained using GWO-PSO is superior in terms of reduction in $V_{D,}$ P_{Loss}, $Q_{Loss,}$ $SCLL_{Current}$, and $R_{S,}$ along with increments in economic benefit. Hence, it can be seen that the proposed methodology for the concurrent optimal planning of multiple DGs (Solar-DG and DSTATCOM) in IEEE 33 and 69-bus reconfigured RDN using APSO and GWO-PSO is productive from the viewpoint of reduction in real power loss and reactive power loss and improvement in the voltage profile, as well as the short circuit level of line current, and its reliability.

Author Contributions: Conceptualization, B.K.S.; methodology, B.K.S.; software, B.K.S.; validation, B.K.S., A.K.B., J.H.J. and M.L.K.; formal analysis, B.K.S.; investigation, B.K.S.; resources, B.K.S.; data curation, B.K.S.; writing—original draft preparation, B.K.S.; writing—review and editing, B.K.S.; visualization, B.K.S.; supervision, A.K.B. and M.L.K. All authors have read and agreed to the published version of the manuscript.

Funding: This research received no external funding.

Institutional Review Board Statement: This study did not require ethical approval.

Acknowledgments: All the authors acknowledge the NIT-Durgapur and the Ministry of Education Government of India, for giving the facility to conduct the research.

Conflicts of Interest: The authors declare no conflict of interest.

Abbreviations and Acronyms

DG	Distributed Generation
Solar-DG/RDG	Renewable Distributed Generation
RDN	Radial Distribution Network
DSTATCOM	Distribution STATic COMpensator
TS	Reconfiguration Tie-Switching
APSO	Adaptive Particle Swarm Optimization
GWO-PSO	Grey Wolf-Particle Swarm Optimization
P_{Loss}	Real Power Loss
Q_{Loss}	Reactive Power Loss
V_D	Deviation of Voltage
$SCLL_{Current}$	Short Circuit level of Line Current
R_S	System Reliability
MO_F^F	Multiple-objective based fitness-function
IP_{Loss}	Index for Real Power Loss
IQ_{Loss}	Index for Reactive Power Loss
IV_D	Index for Deviation of Voltage
$ISCLL_{Current}$	Index for Short Circuit level of Line Current
IR_S	Index for System Reliability
SAIFI	System Average Interruption Frequency Index
SAIDI	System Average Interruption Duration Index
CAIDI	Customer Average Interruption Duration Index
ENS	Energy Not Supplied
P_{RDG}	Solar-DG size as Real Power DG
Q_{DSTAT}	DSTATCOM size as Reactive Power DG
P_{SB_GEN}	Real Power Generation at Slack Bus
Q_{SB_GEN}	Reactive Power Generation at Slack Bu
C_{Load}, VR_{Load}	Constant Load, Variable load
IN_{Load}, RES_{Load}	Industrial Load, Residential Load
COM_{Load}, MIX_{Load}	Commercial Load, Mixed Load

References

1. Oda, E.S.; El Hamed, A.M.A.; Ali, A.; Elbaset, A.A.; El Sattar, M.A.; Ebeed, M. Stochastic Optimal Planning of Distribution System Considering Integrated Photovoltaic-Based DG and DSTATCOM Under Uncertainties of Loads and Solar Irradiance. *IEEE Access* **2021**, *9*, 26541–26555. [CrossRef]
2. Isha, G.; Jagatheeswari, P. Optimal allocation of DSTATCOM and PV array in distribution system employing fuzzy-lightning search algorithm. *Automatika* **2021**, *62*, 339–352. [CrossRef]
3. Ghatak, S.R.; Sannigrahi, S.; Acharjee, P. Comparative performance analysis of DG and DSTATCOM using improved PSO based on success rate for deregulated environment. *IEEE Syst. J.* **2017**, *12*, 2791–2802. [CrossRef]
4. Sannigrahi, S.; Ghatak, S.R.; Acharjee, P. Strategically incorporation of RES and DSTATCOM for techno-economic-environmental benefits using search space reduction-based ICSA. *IET Gener. Transm. Distrib.* **2019**, *13*, 1369–1381. [CrossRef]
5. Yuvaraj, T.; Ravi, K.; Devabalaji, K.R. Optimal allocation of DG and DSTATCOM in radial distribution system using cuckoo search optimization algorithm. *Model. Simul. Eng.* **2017**, *2017*, 2857926. [CrossRef]
6. Sannigrahi, S.; Ghatak, S.R.; Acharjee, P. Fuzzy logic–based rooted tree optimization algorithm for strategic incorporation of DG and DSTATCOM. *Int. Trans. Electr. Energy Syst.* **2019**, *29*, e12031. [CrossRef]
7. Yuvaraj, T.; Ravi, K.; Devabalaji, K.R. DSTATCOM allocation in distribution networks considering load variations using bat algorithm. *Ain Shams Eng. J.* **2017**, *8*, 391–403. [CrossRef]
8. Tolabi, H.B.; Ali, M.H.; Rizwan, M. Simultaneous reconfiguration, optimal placement of DSTATCOM, and photovoltaic array in a distribution system based on fuzzy-ACO approach. *IEEE Trans. Sustain. Energy* **2014**, *6*, 210–218. [CrossRef]
9. Ghatak, S.R.; Sannigrahi, S.; Acharjee, P. Multiobjective Framework for Optimal Integration of Solar Energy Source in Three-Phase Unbalanced Distribution Network. *IEEE Trans. Ind. Appl.* **2020**, *56*, 3068–3078. [CrossRef]
10. Malik, M.Z.; Kumar, M.; Soomro, A.M.; Baloch, M.H.; Farhan, M.; Gul, M.; Kaloi, G.S. Strategic planning of renewable distributed generation in radial distribution system using advanced MOPSO method. *Energy Rep.* **2020**, *6*, 2872–2886. [CrossRef]
11. Thangaraj, Y.; Kuppan, R. Multi-objective simultaneous placement of DG and DSTATCOM using novel lightning search algorithm. *J. Appl. Res. Technol.* **2017**, *15*, 477–491. [CrossRef]
12. Weqar, B.; Khan, M.T.; Siddiqui, A.S. Optimal placement of distributed generation and D-STATCOM in radial distribution network. *Smart Sci.* **2018**, *6*, 125–133. [CrossRef]

13. Salkuti, S.R. Optimal allocation of DG and D-STATCOM in a distribution system using evolutionary based Bat algorithm. *Int. J. Adv. Comput. Sci. Appl. (IJACSA)* **2021**, *12*, 360–365. [CrossRef]
14. Sambaiah, K.S.; Jayabarathi, T. Optimal reconfiguration of distribution network in presence of D-STATCOM and photovoltaic array using a metaheuristic algorithm. *Eur. J. Electr. Eng. Comput. Sci.* **2020**, *4*, 1–15. [CrossRef]
15. Yuvaraj, T.; Ravi, K. Multi-objective simultaneous DG and DSTATCOM allocation in radial distribution networks using cuckoo searching algorithm. *Alex. Eng. J.* **2018**, *57*, 2729–2742. [CrossRef]
16. Chinnaraj, S.G.R.; Kuppan, R. Optimal sizing and placement of multiple renewable distribution generation and DSTATCOM in radial distribution systems using hybrid lightning search algorithm-simplex method optimization algorithm. *Comput. Intell.* **2021**, *37*, 1673–1690. [CrossRef]
17. Injeti, S.K.; Thunuguntla, V.K. Optimal integration of DGs into radial distribution network in the presence of plug-in electric vehicles to minimize daily active power losses and to improve the voltage profile of the system using bio-inspired optimization algorithms. *Prot. Control. Mod. Power Syst.* **2020**, *5*, 1–15. [CrossRef]
18. Balu, K.; Mukherjee, V. Optimal siting and sizing of distributed generation in radial distribution system using a novel student psychology-based optimization algorithm. *Neural Comput. Appl.* **2021**, *33*, 15639–15667. [CrossRef]
19. Mirjalili, S.; Mirjalili, S.M.; Lewis, A. Grey wolf optimizer. *Adv. Eng. Softw.* **2014**, *69*, 46–61. [CrossRef]
20. Gohil, B.N.; Patel, D.R. A hybrid GWO-PSO algorithm for load balancing in cloud computing environment. In Proceedings of the 2018 Second International Conference on Green Computing and Internet of Things (ICGCIoT), Bangalore, India, 16–18 August 2018.
21. Kraiem, H.; Aymen, F.; Yahya, L.; Triviño, A.; Alharthi, M.; Ghoneim, S.S.M. A comparison between particle swarm and grey wolf optimization algorithms for improving the battery autonomy in a photovoltaic system. *Appl. Sci.* **2021**, *11*, 7732. [CrossRef]
22. Şenel, F.A.; Gökçe, F.; Yüksel, A.S.; Yiğit, T. A novel hybrid PSO–GWO algorithm for optimization problems. *Eng. Comput.* **2019**, *35*, 1359–1373. [CrossRef]
23. Ackermann, T.; Andersson, G.; Söder, L. Distributed generation: A definition. *Electr. Power Syst. Res.* **2001**, *57*, 195–204. [CrossRef]
24. Teng, J.-H. A direct approach for distribution system load flow solutions. *IEEE Trans. Power Deliv.* **2003**, *18*, 882–887. [CrossRef]
25. Díaz, G.; Gómez-Aleixandre, J.; Coto, J. Direct backward/forward sweep algorithm for solving load power flows in AC droop-regulated microgrids. *IEEE Trans. Smart Grid* **2015**, *7*, 2208–2217. [CrossRef]
26. Alam, A.; Gupta, A.; Bindal, P.; Siddiqui, A.; Zaid, M. Power loss minimization in a radial distribution system with distributed generation. In Proceedings of the 2018 International Conference on Power, Energy, Control and Transmission Systems (ICPECTS), Chennai, India, 22–23 February 2018.
27. Kennedy, J.; Eberhart, R. Particle swarm optimization. In Proceedings of the ICNN'95-International Conference on Neural Networks, Perth, WA, Australia, 27 November–1 December 1995; Volume 4.
28. Zhan, Z.H.; Zhang, J.; Li, Y.; Chung, H.S.H. Adaptive particle swarm optimization. *IEEE Trans. Syst. Man Cybern. Part B (Cybern.)* **2009**, *39*, 1362–1381. [CrossRef]
29. Dulău, L.I.; Abrudean, M.; Bică, D. Distributed generation technologies and optimization. *Procedia Technol.* **2014**, *12*, 687–692. [CrossRef]
30. Bohre, A.K.; Agnihotri, G.; Dubey, M. Optimal sizing and sitting of DG with load models using soft computing techniques in practical distribution system. *IET Gener. Transm. Distrib.* **2016**, *10*, 2606–2621. [CrossRef]
31. El-Zonkoly, A.M. Optimal placement of multi-distributed generation units including different load models using particle swarm optimisation. *IET Gener. Transm. Distrib.* **2011**, *5*, 760–771. [CrossRef]
32. Ochoa, L.F.; Padilha-Feltrin, A.; Harrison, G.P. Evaluating distributed time-varying generation through a multiobjective index. *IEEE Trans. Power Deliv.* **2008**, *23*, 1132–1138. [CrossRef]
33. Prakash, R.; Sujatha, B.C. Optimal placement and sizing of DG for power loss minimization and VSI improvement using bat algorithm. In Proceedings of the 2016 National Power Systems Conference (NPSC), Bhubaneswar, India, 19–21 December 2016.
34. Sedighizadeh, M.; Esmaili, M.; Mahmoodi, M.M. Reconfiguration of distribution systems to improve reliability and reduce power losses using imperialist competitive algorithm. *Iran. J. Electr. Electron. Eng.* **2017**, *13*, 287–302.
35. Prakash, D.; Lakshminarayana, C. Multiple DG placements in distribution system for power loss reduction using PSO algorithm. *Procedia Technol.* **2016**, *25*, 785–792. [CrossRef]
36. Zimmerman, R.D.; Murillo-Sanchez, C.E. 'Matpower7.1', October 2020. Available online: http://www.pserc.cornell.edu//matpower/ (accessed on 1 October 2022).
37. Swarnkar, A.; Gupta, N.; Niazi, K. A novel codification for meta-heuristic techniques used in distribution network reconfiguration. *Electr. Power Syst. Res.* **2011**, *81*, 1619–1626. [CrossRef]
38. Reddy, A.S.; Reddy, M.D. Optimization of network reconfiguration by using particle swarm optimization. In Proceedings of the 2016 IEEE 1st International Conference on Power Electronics, Intelligent Control and Energy Systems (ICPEICES), Delhi, India, 4–6 July 2016.
39. Hien, N.C.; Mithulananthan, N.; Bansal, R.C. Location and sizing of distributed generation units for loadabilty enhancement in primary feeder. *IEEE Syst. J.* **2013**, *7*, 797–806. [CrossRef]
40. Hung, D.Q.; Mithulananthan, N. Multiple distributed generator placement in primary distribution networks for loss reduction. *IEEE Trans. Ind. Electron.* **2011**, *60*, 1700–1708. [CrossRef]

41. Hung, D.Q.; Mithulananthan, N.; Bansal, R.C. Analytical expressions for DG allocation in primary distribution networks. *IEEE Trans. Energy Convers.* **2010**, *25*, 814–820. [CrossRef]
42. Georgilakis, P.S.; Hatziargyriou, N.D. Optimal distributed generation placement in power distribution networks: Models, methods, and future research. *IEEE Trans. Power Syst.* **2013**, *28*, 3420–3428. [CrossRef]
43. Sawle, Y.; Gupta, S.; Bohre, A.K. Review of hybrid renewable energy systems with comparative analysis of off-grid hybrid system. *Renew. Sustain. Energy Rev.* **2018**, *81*, 2217–2235. [CrossRef]
44. Lujano-Rojas, J.M.; Dufo-Lopez, R.; Bernal-Agustín, J.L. Technical and economic effects of charge controller operation and coulombic efficiency on stand-alone hybrid power systems. *Energy Convers. Manag.* **2014**, *86*, 709–716. [CrossRef]
45. Olatomiwa, L.; Mekhilef, S.; Huda, A.; Ohunakin, O.S. Economic evaluation of hybrid energy systems for rural electrification in six geo-political zones of Nigeria. *Renew. Energy* **2015**, *83*, 435–446. [CrossRef]
46. Giraud, F.; Salameh, Z.M. Steady-state performance of a grid-connected rooftop hybrid wind-photovoltaic power system with battery storage. *IEEE Trans. Energy Convers.* **2001**, *16*, 1–7. [CrossRef]
47. Ghatak, S.R.; Sannigrahi, S.; Acharjee, P. Multi-objective approach for strategic incorporation of solar energy source, battery storage system, and DSTATCOM in a smart grid environment. *IEEE Syst. J.* **2018**, *13*, 3038–3049. [CrossRef]
48. Taher, S.A.; Afsari, S.A. Optimal location and sizing of DSTATCOM in distribution systems by immune algorithm. *Int. J. Electr. Power Energy Syst.* **2014**, *60*, 34–44. [CrossRef]
49. Hosseini, M.; Shayanfar, H.A. Regular paper modeling of series and shunt distribution FACTS devices in distribution systems load flow. *J. Electr. Syst.* **2008**, *4*, 1–12.
50. Acha, E.; Fuerte-Esquivel, C.R.; Ambriz-Perez, H.; Angeles-Camacho, C. *FACTS: Modelling and Simulation in Power Networks*; John Wiley & Sons: Hoboken, NJ, USA, 2004.
51. Kadir, A.F.A.; Mohamed, A.; Shareef, H.; Wanik, M.Z.C. Optimal placement and sizing of distributed generations in distribution systems for minimizing losses and THD_v using evolutionary programming. *Turk. J. Electr. Eng. Comput. Sci.* **2013**, *21* (Suppl. S2), 2269–2282. [CrossRef]
52. Vempalle, R.; Dhal, P.K. Optimal Placement of Distributed Generators in Optimized Reconfigure. Radial Distribution Network using PSO-DA Optimization Algorithm. In Proceedings of the 2020 International Conference on Advances in Computing, Communication & Materials (ICACCM), Dehradun, India, 21–22 August 2020.
53. Muhammad, M.A.; Mokhlis, H.; Naidu, K.; Amin, A.; Franco, J.F.; Othman, M. Distribution network planning enhancement via network reconfiguration and DG integration using dataset approach and water cycle algorithm. *J. Mod. Power Syst. Clean Energy* **2019**, *8*, 86–93. [CrossRef]
54. Rahim, M.N.A.; Mokhlis, H.; Abu Bakar, A.H.; Rahman, M.T.; Badran, O.; Mansor, N.N. Protection coordination toward optimal network reconfiguration and DG sizing. *IEEE Access* **2019**, *7*, 163700–163718. [CrossRef]